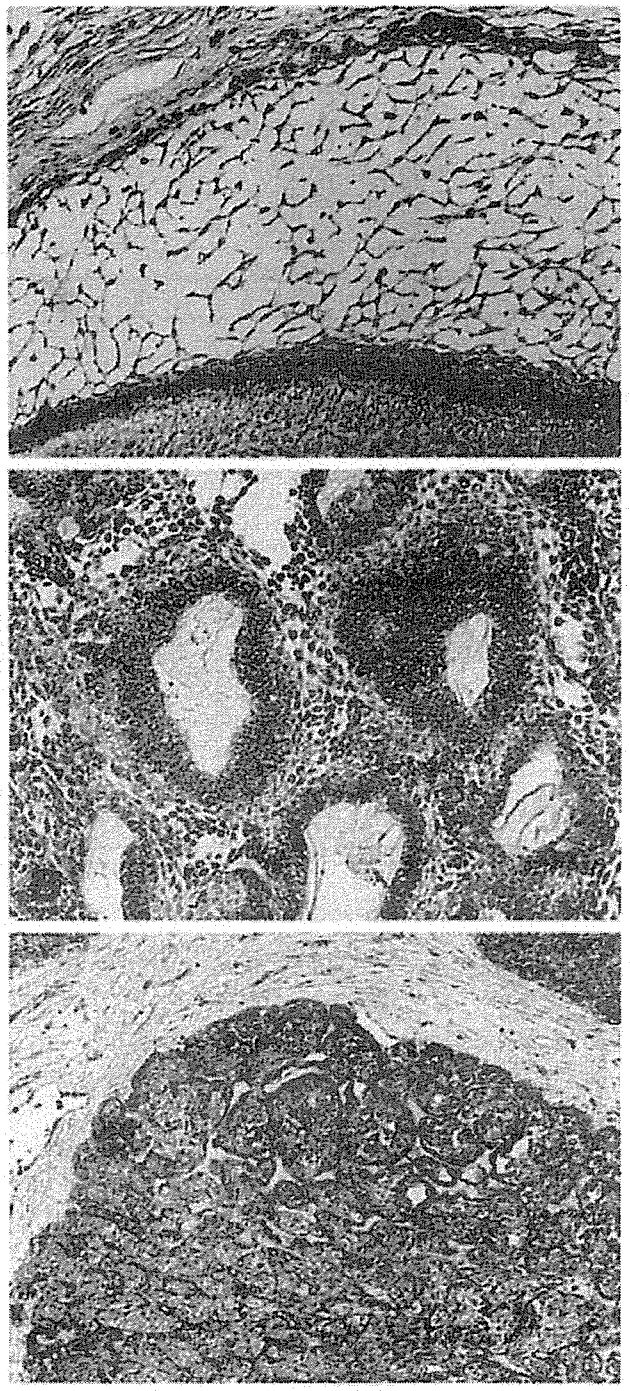

Figure 3 Immunohistochemical reactivity for MEK1. (A) Tooth germ showing strong reactivity in inner enamel epithelium and weak to moderate reactivity in outer enamel epithelium, stratum intermedium and stellate reticulum (×100). (B) Plexiform ameloblastoma showing strong reactivity in peripheral columnar or cuboidal cells and weak to moderate reactivity in central polyhedral cells (×125). (C) Ameloblastic carcinoma showing strong reactivity in most neoplastic cells (×100).

MEK1 expression was detected in most epithelial cells in tooth germs, and reactivity in inner enamel epithelium was stronger than that in other epithelial components (Fig. 3A). Ameloblastomas showed MEK1 expression in most neoplastic cells, and reactivity in peripheral columnar or cuboidal calls was stronger than that in central polyhedral cells (Fig. 3B). Keratinizing cells in acanthomatous ameloblastomas and granular cells in granular cell ameloblastomas demonstrated low reactivity for MEK1. Basal cell ameloblastomas and desmoplastic ameloblastomas showed diffuse MEK1 expression in neoplastic cells. Metastasizing ameloblastomas showed a MEK1 expression pattern similar to that of follicular ameloblastomas, while ameloblastic carcinomas were moderately to strongly positive for MEK1 in most neoplastic cells (Fig. 3C).

Immunohistochemical reactivity for ERK1/2 was detected usually in the cytoplasm and often in the nuclei of normal and neoplastic odontogenic epithelial cells (Fig. 4). In tooth germs, ERK1/2 expression was found in most epithelial cells, and reactivity in inner and outer enamel epithelium was stronger than that in other epithelial components (Fig. 4A). Ameloblastomas showed ERK1/2 expression in most neoplastic cells, and reactivity in peripheral columnar or cuboidal cells was stronger than that in central polyhedral cells. Keratinizing cells in acanthomatous ameloblastomas and granular cells in granular cell ameloblastomas demonstrated markedly decreased reactivity for ERK1/2 (Fig. 4B). Basal cell ameloblastomas and desmoplastic ameloblastomas showed diffuse ERK1/2 expression in neoplastic cells. Metastasizing ameloblastomas showed a ERK1/2 expression pattern similar to that of follicular ameloblastomas, while ameloblastic carcinomas were moderately to strongly positive for ERK1/2 in most neoplastic cells (Fig. 4C).

*Mutation analysis of K-*Ras *gene*

Direct DNA sequencing for K-*Ras* gene mutations was carried out in 22 ameloblastomas (13 follicular and 9 plexiform cases, including 7 acanthomatous, 3 granular cell, 1 basal cell and 1 desmoplastic subtypes) and 1 malignant ameloblastoma (1 metastasizing ameloblastoma). A GGT to GCT (glycine to alanine) point mutation was detected at codon 12 in exon 1 of K-*Ras* gene in one follicular ameloblastoma without cellular subtype (Fig. 5). Mutational alteration was not detected at codon 13 in exon 1 or codon 61 in exon 2 of K-*Ras* gene in any of the 23 cases.

Discussion

RAS/MAPK signaling pathway is a primordial signaling system that controls such fundamental cellular processes as cell proliferation and differentiation (16, 18). Mouse embryos homozygous for K-*Ras* mutation die *in utero*, suggesting that K-*Ras* is essential for embryogenesis (33). Expression of Raf1 is recognized in various mouse fetal tissues (34). MEK1 and ERK are known to be necessary for PC12 cell neuronal differentiation (35, 36). These features suggest that Ras/MAPK signaling pathway plays a role in cellular regulation during developmental processes (34–36). Raf-1 expression has been detected at different stages of mouse tooth

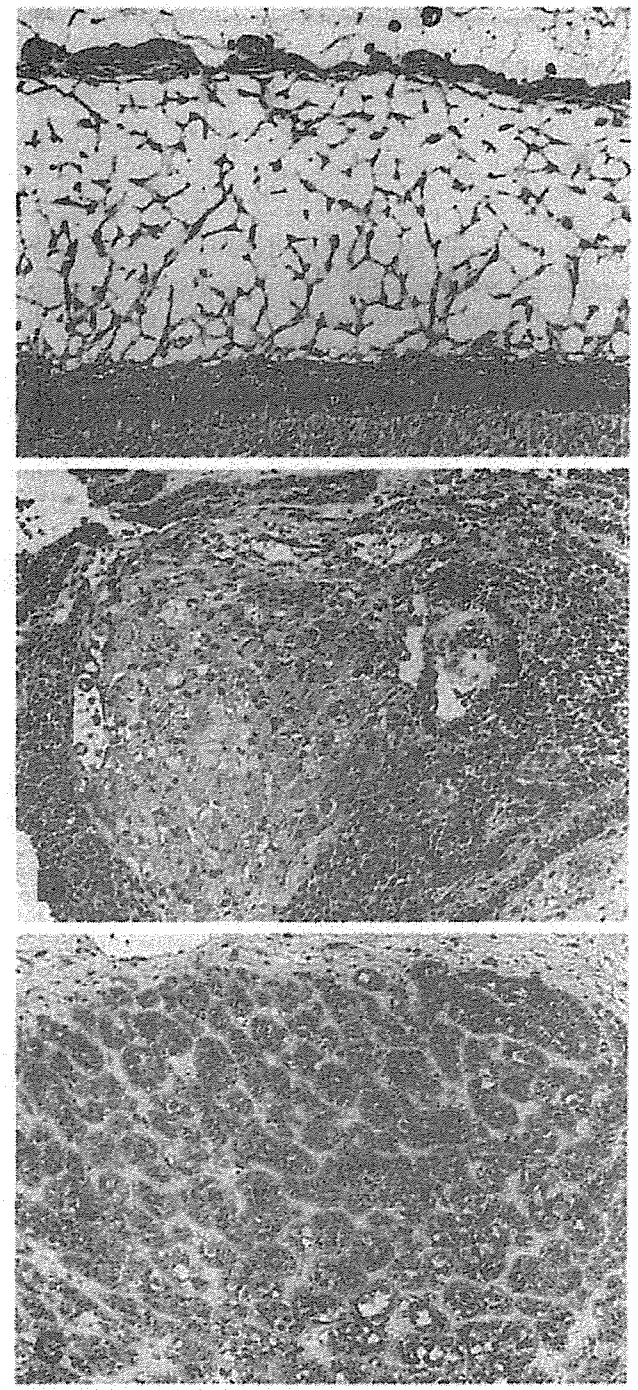

Figure 4 Immunohistochemical reactivity for ERK1/2. (A) Tooth germ showing strong reactivity in inner and outer enamel epithelium and weak to moderate reactivity in stratum intermedium and stellate reticulum (×125). (B) Granular cell ameloblastoma showing marked reactivity in peripheral cuboidal cells and central polyhedral cells and decreased reactivity in granular cells (×95). (C) Ameloblastic carcinoma showing strong reactivity in most neoplastic cells (×115).

germ development (31), and ERK reactivity has been studied in odontogenic epithelial rests neighboring human odontogenic cysts (32). In the present study,

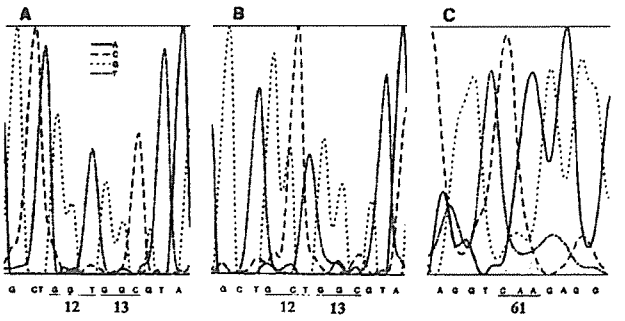

Figure 5 Direct DNA sequencing of K-*Ras* gene in ameloblastoma. (A) No mutation at codons 12 and 13 in exon 1. (B) A GGT to GCT point mutation at codon 12 in exon 1. (C) No mutation at codon 61 in exon 2.

Ras/MAPK signaling molecules were detected in epithelial components of tooth germs at the initial stage of crown mineralization. These features suggest that Ras signaling plays a role in cell proliferation and differentiation during tooth development.

Ras signaling functions as a relay switch in downstream of cell surface receptor tyrosine kinases, including receptors for many growth factors, such as epidermal (EGF), hepatocyte (HGF), platelet-derived (PDGF), insulin-like (IGF), fibroblast (FGF), vascular endothelial (VEGF), and nerve (NGF) growth factors (17, 18). Receptors for EGF, FGF, and HGF have been investigated in odontogenic tumors, suggesting that these receptor tyrosine kinases affect cell proliferation in oncogenesis or malignant transformation of odontogenic epithelium (29, 37–39). Aberrant expression and/or activation of signal transducing proteins are linked with neoplastic change (16, 20, 22). Alterations in Ras/MAPK signaling pathway, such as overexpression or constitutive activation of signaling molecules, have been detected in various malignancies, including lung, renal, prostate, breast, ovarian, and oral carcinomas (19, 21, 23, 40–42). Overexpression of $p21^{Ras}$ in ameloblastomas and activation of ERK in odontogenic cysts are related to the biological behavior of the odontogenic lesions (30, 32). In the present study, ameloblastomas expressed Ras/MAPK signaling molecules evidently in peripheral neoplastic cells, and basal cell ameloblastomas tended to show stronger reactivity for the signaling molecules than did the other subtypes. These features suggest that Ras/MAPK signaling pathway plays a role in promoting the proliferation of ameloblastoma cells. However, expression of Ras/MAPK signaling molecules in ameloblastomas did not clearly differ from that in tooth germs or malignant ameloblastomas. K-Ras immunoreactivity in malignant ameloblastomas was lower than that in dental lamina of tooth germs, whereas no apparent difference was found in reactivity for Raf1, MEK1, or ERK1/2 between tooth germs and malignant ameloblastomas. These results did not clearly show that these molecules have a specific role in oncogenesis or malignant transformation of odontogenic epithelium. In this study, expression of Ras/MAPK signaling molecules in plexiform ameloblastomas was slightly stronger than that in

follicular ameloblastomas. Keratinizing cells and granular cells showed decreased reactivity for the signaling molecules in acanthomatous and granular cell ameloblastomas. These features suggest that Ras/MAPK signaling might play a role in tissue structuring and/or cytodifferentiation of ameloblastomas.

A series of genetic alterations appear to promote the development of tumors via multiple steps (13, 43). Point mutations at codons 12, 13, and 61 of K-*Ras* gene are found in approximately 30% of solid tumors, and the incidences of these mutations are high in pancreatic, colorectal, lung, ovarian, and endometrial carcinomas (13, 14, 44–46). Mutated Ras product constitutively transduces signals and promotes cellular proliferation (10, 16). In the present study using direct DNA sequencing, a point mutation of K-*Ras* was detected at codon 12 in only 1 of 22 ameloblastomas and 1 metastasizing ameloblastoma, suggesting that K-*Ras* mutation might play a minor role in neoplastic change of odontogenic epithelium. Our immunohistochemical examination revealed relatively low reactivity for K-Ras product in ameloblastic carcinomas; however, mutation analysis of K-*Ras* gene in ameloblastic carcinomas could not be investigated because of the rarity of this malignancy. Further studies should be carried out to determine the association between K-*Ras* and the malignant potential of odontogenic epithelium.

References

1. Kramer IRH, Pindborg JJ, Shear M. *WHO Histological Typing of Odontogenic Tumours.* Berlin: Springer-Verlag, 1992; 11–27.
2. Melrose RJ. Benign epithelial odontogenic tumors. *Semin Diagn Pathol* 1999; **16**: 271–87.
3. Eversole LR. Malignant epithelial odontogenic tumors. *Semin Diagn Pathol* 1999; **16**: 317–24.
4. Sciubba JJ, Fantasia JE, Kahn LB. *Tumors and Cysts of the Jaw.* Washington, DC: Armed Forces institute of Pathology, 2001: 71–99.
5. Heikinheimo K, Jee KJ, Niini T, et al. Gene expression profiling of ameloblastoma and human tooth germ by means of a cDNA microarray. *J Dent Res* 2002; **81**: 525–30.
6. Jaakelainen K, Jee KJ, Leivo I, Saloniemi I, Knuutila S, Heikinheimo K. Cell proliferation and chromosomal changes in human ameloblastoma. *Cancer Genet Cytogenet* 2002; **136**: 31–7.
7. Shibata T, Nakata D, Chiba I, et al. Detection of TP53 mutation in ameloblastoma by the use of a yeast functional assay. *J Oral Pathol Med* 2002; **31**: 534–8.
8. Der CJ, Krontiris TG, Cooper GM. Transforming genes of human bladder and lung carcinoma cell lines are homologous to the *ras* genes of Harvey and Kirsten sarcoma viruses. *Proc Natl Acad Sci USA* 1982; **79**: 3637–40.
9. Shimizu K, Goldfarb M, Suard Y, et al. Three human transforming genes are related to the viral *ras* oncogenes. *Proc Natl Acad Sci USA* 1983; **80**: 2112–6.
10. Barbacid M. *ras* genes. *Ann Rev Biochem* 1987; **56**: 779–827.
11. Capon DJ, Seeburg PH, McGrath JP, et al. Activation of Ki-ras2 gene in human colon and lung carcinomas by two different point mutations. *Nature* 1983; **304**: 507–13.
12. Almoguera C, Shibata D, Forrester K, Martin J, Arnheim N, Perucho M. Most human carcinomas of the exocrine pancreas contain mutant c-K-*ras* genes. *Cell* 1988; **53**:549–54.
13. Vogelstein B, Fearon ER, Hamilton SR, et al. Genetic alterations during colorectal-tumor development. *N Engl J Med* 1988; **319**: 525–32.
14. Bos JL. *ras* oncogenes in human cancer: a review. *Cancer Res* 1989; **49**: 4682–9.
15. White MA, Nicolette C, Minden A, et al. *Cell* 1995; **80**: 533–41.
16. Seger R, Krebs EG. The MAPK signaling cascade. *FASEB J* 1995; **9**: 726–35.
17. Marshall CJ. Specificity of receptor tyrosine kinase signaling: transient versus sustained extracellular signal-regulated kinase activation. *Cell* 1995; **80**: 179–85.
18. Kolch W. Meaningful relationships. the regulation of the Ras/Raf/MEK/ERK pathway by protein interactions. *Biochem J* 2000; **351**: 289–305.
19. Hajj C, Akoum R, Bradley E, Paquin F, Ayoub J. DNA alterations at proto-oncogene loci and their clinical significance in operable non-small cell lung cancer. *Cancer* 1990; **66**: 733–9.
20. Gulbis B, Galand P. Immunodetection of the p21-*ras* products in human normal and preneoplastic tissues and solid tumors: a review. *Hum Pathol* 1993; **24**: 1271–85.
21. Oka H, Chatani Y, Hoshino R, et al. Constitutive activation of mitogen-activated protein (MAP) kinases in human renal cell carcinoma. *Cancer Res* 1995; **55**: 4182–7.
22. Hoshino R, Chatani Y, Tamori T, et al. Constitutive activation of the 41-/43-kDa mitogen-activated protein kinase signaling pathway in human tumors. *Oncogene* 1999; **18**: 813–22.
23. Albanell J, Codony-Sevat J, Rojo F, et al. Activated extracellular signal–regulated kinases: association with epidermal growth factor receptor/transforming growth factor α expression in head and heck squamous carcinoma and inhibition by anti-epidermal growth factor receptor treatments. *Cancer Res* 2001; **61**: 6500–10.
24. Kumamoto H. Detection of apoptosis-related factors and apoptotic cells in ameloblastomas. analysis by immunohistochemistry and an in situ DNA nick end-labelling method. *J Oral Pathol Med* 1997; **26**: 419–25.
25. Kumamoto H, Ooya K. Immunohistochemical analysis of bcl-2 family proteins in benign and malignant ameloblastomas. *J Oral Pathol Med* 1999; **28**: 343–9.
26. Kumamoto H, Kimi K, Ooya K. Immunohistochemical analysis of apoptosis-related factors (Fas, Fas ligand, caspase-3 and single-stranded DNA) in ameloblastomas. *J Oral Pathol Med* 2001; **30**: 596–602.
27. Kumamoto H, Kinouchi Y, Ooya K. Telomerase activity and telomerase reverse transcriptase (TERT) expression in ameloblastomas. *J Oral Pathol Med* 2001; **30**: 231–6.
28. Kumamoto H, Kimi K, Ooya K. Detection of cell cycle-related factors in ameloblastomas. *J Oral Pathol Med* 2001; **30**: 309–15.
29. Kumamoto H, Yoshida M, Ooya K. Immunohistochemical detection of hepatocyte growth factor, transforming growth factor-β and their receptors in epithelial odontogenic tumors. *J Oral Pathol Med* 2002; **31**: 539–48.
30. Sandros J, Heikinheimo K, Happonen R-P, Stenman G. Expression of p21RAS in odontogenic tumors. *APMIS* 1991; **99**: 15–20.
31. Sunohara M, Tanzawa H, Kaneko Y, Fuse A, Sato K. Expression patterns of Raf-1 suggest multiple roles in tooth development. *Calcif Tissue Int* 1996; **58**: 60–4.
32. Nickolaychuk B, McNicol A, Gilchrist J, Birek C. Evidence for a role of mitogen-activated protein kinases in proliferating and differentiating odontogenic epithelia

of inflammatory and developmental cysts. *Oral Surg Oral Med Oral Pathol Oral Radiol Endod* 2002; **93**: 720–9.
33. Johnson L, Greenbaum D, Cichowski K, et al. K-*ras* is an essential gene in the mouse with partial functional overlap with N-*ras*. *Genes Dev* 1997; **11**: 2468–81.
34. Storm SM, Cleveland JL, Rapp UR. Expression of *raf* family proto-oncogenes in normal mouse tissues. *Oncogene* 1990; **5**: 345–51.
35. Qui M-S, Green SH. PC12 cell neuronal differentiation is associated with prolonged $p21^{ras}$ activity and consequent prolonged ERK activity. *Neuron* 1992; **9**: 705–17.
36. Cowley S, Paterson H, Kemp P, Marchall C. Activation of MAP kinase kinase is necessary and sufficient for PC12 differentiation and for transformation of NIH 3T3 cells. *Cell* 1994; **77**: 841–52.
37. Shrestha P, Yamada K, Higashiyama H, Takagi H, Mori M. Epidermal growth factor receptor in odontogenic cysts and tumors. *J Oral Pathol Med* 1992; **21**: 314–7.
38. Heikinheimo K, Voutilainen R, Happonen R-P, Miettinen PJ. EGF receptor and its ligands, EGF and TGF-α, in developing and neoplastic human odontogenic tissues. *Int J Dev Biol* 1993; **37**: 387–96.
39. So F, Daley TD, Jackson L, Wysocki GP. Immunohistochemical localization of fibroblast growth factors FGF-1 and FGF-2, and receptors FGFR2 and FGFR3 in the epithelium of human odontogenic cysts and tumors. *J Oral Pathol Med* 2001; **30**: 428–33.
40. Sivaraman VS, Wang H-Y, Nuovo GJ, Malbon CC. Hyperexpression of mitogen-activated protein kinase in human breast cancer. *J Clin Invest* 1997; **99**: 1478–83.
41. Magi-Galluzzi C, Mishra R, Fiorentino M, et al. Mitogen-activated protein kinase phosphatase 1 is overexpressed in prostate cancers and is inversely relate to apoptosis. *Laboratory Invest* 1997; **76**: 37–51.
42. Kupryjanczyk J, Szymanska T, Madry R, et al. Evaluation of clinical significance of TP53, BCL-2, BAX and MEK1 expression in 229 ovarian carcinomas treated with platinum-based regimen. *Br J Cancer* 2003; **88**: 848–54.
43. Fearon ER, Vogelstein. A genetic model for colorectal tumorigenesis. *Cell* 1990; **61**: 759–67.
44. Forrester K, Almoguera C, Han K, Grizzle WE, Peruch M. Detection of high incidence of K-*ras* oncogenes during human colon tumorigenesis. *Nature* 1987; **327**: 298–303.
45. Enomoto T, Weghorst CM, Inoue M, Tanizawa O, Rice JM. K-*ras* activation occurs frequently in mucinous adenocarcinomas and rarely in other common epithelial tumors of the human ovary. *Am J Pathol* 1991; **139**: 777–85.
46. Imamura T, Arima T, Kato H, Miyamoto S, Sasazuki T, Wake N. Chromosomal deletions and K-*ras* gene mutations in human endometrial carcinomas. *Int J Cancer* 1992; **51**: 47–52.

Original Paper

Caries Research

Caries Res 2004;38:448–453
DOI: 10.1159/000079626

Received: April 2, 2003
Accepted after revision: November 25, 2003

A Method for Mapping the Distribution Pattern of Cariogenic Streptococci within Dental Plaque in vivo

K. Kato[a] T. Sato[b] N. Takahashi[b] K. Fukui[a] K. Yamamoto[a] H. Nakagaki[a]

[a]Department of Preventive Dentistry and Dental Public Health, School of Dentistry, Aichi-Gakuin University, Nagoya, and [b]Division of Oral Ecology and Biochemistry, Department of Oral Biology, Tohoku University Graduate School of Dentistry, Sendai, Japan

Key Words

Dental plaque · Distribution of microorganisms · Nested polymerase chain reaction · *Streptococcus mutans* · *Streptococcus sobrinus*

Abstract

This study was carried out to develop a method for mapping the distribution of cariogenic oral streptococci, *Streptococcus mutans* and *Streptococcus sobrinus*, from the outermost to the innermost plaque. Ten consenting subjects were asked to form plaque by abstaining from tooth brushing over 3 days within in situ plaque-generating devices, which were placed on the upper molars. The plaque formed in the devices was separated into 8–10 layered fractions (100 μm thick). Genomic DNA was extracted from each plaque fraction by a commercial DNA purification kit and used for the amplification of the 16S ribosomal RNA gene sequences by polymerase chain reaction (PCR) with universal primers. The products were then amplified by PCR with *S. mutans*- or *S. sobrinus*-specific nested primers. The final products were separated on agarose gels, stained and photographed to confirm the existence of *S. mutans* and *S. sobrinus*. The results showed that *S. mutans* was detected in the plaque obtained from all of the 10 subjects and *S. sobrinus* in the plaque of 7 subjects. However, the distribution patterns of fractions positive for *S. mutans* and *S. sobrinus* varied among the subjects, with a tendency for frequent detection of both species in the outer to middle layers of dental plaque. There were no plaque fractions in which only *S. sobrinus* was found. This method could be useful to map the distribution of cariogenic microorganisms and to estimate the bacterial ecology for oral biofilm.

Dental plaque is the tooth-associated biofilm consisting of a microbial community and a matrix of polymer of bacterial and host origin, and is also found on the various restorative materials introduced by dental treatment. Dental plaque plays a primary role in the etiology of dental caries, so their biological and cariogenic properties are basic to caries prevention. Mutans streptococci including *Streptococcus mutans* and *Streptococcus sobrinus* have been well known as the group of oral microorganisms which have virulence factors related to cariogenicity. They drop the plaque pH to low levels by producing acids from carbohydrates and survive in this acidic environment. They also produce extracellular polysaccharides which may promote the dissolution of the tooth surfaces by increasing the porosity of plaque matrix and permitting deeper penetration of sugar [Dibdin and Shellis, 1988; Cury et al., 2000]. Epidemiological studies have provided strong evidence of the relationship between the levels of mutans streptococci and the development of caries [Lang et al., 1987; Roeters et al., 1995]. In addition,

KARGER

Fax + 41 61 306 12 34
E-Mail karger@karger.ch
www.karger.com

0008–6568/04/0385–0448$21.00/0

Accessible online at:
www.karger.com/cre

Dr. Kazuo Kato, Department of Preventive Dentistry and
Dental Public Health, School of Dentistry, Aichi-Gakuin University
1-100 Kusumoto-cho, Chikusa-ku, Nagoya 464-8650 (Japan)
Tel. +81 52 751 2561, ext. 352, Fax +81 52 752 5988
E-Mail kazkato@dpc.aichi-gakuin.ac.jp

their early acquisition by children is positively correlated with white spot lesions or lesions with cavitation [Köhler et al., 1988; Caufield et al., 1993; Milgrom et al., 2000]. Therefore, the levels of mutans streptococci in plaque [Milgrom et al., 2000; Pienihäkkinen and Jokela, 2002] and saliva [Jensen and Bratthall, 1989] are considered to be important indicators for assessment of caries risk or management of caries prevention.

Dental plaque is a watery and frail heterogeneous complex material accumulating on the teeth. As dental plaque accumulates and matures, the depth-specific microbial differences in dental plaque may increase, depending on several physiological factors such as the oxygen concentration, pH, and nutrient availability. However, little attention has been paid to the detection or the identification of plaque bacteria relating to the structure of plaque on the tooth surface.

Several attempts have been made to clarify the location of specific bacteria in plaque. Ritz [1969] applied immunofluorescent staining of plaque sections to demonstrate the spatial relationship between aerobic and anaerobic bacteria in the plaque. This technique has often been used to detect periodontal pathogens in the apical plaque border [Christersson et al., 1987]. Noiri et al. [2001] found periodontal disease-associated bacteria in the periodontal tissue surrounding the roots of teeth that were extracted from periodontitis patients. Recently, a confocal laser scanning microscope (CLSM) has also been applied to study the relationship between the spatial structure of smooth surface plaque and the microbial ecology [Wood et al., 2000; Auschill et al., 2001].

We have reported on the fluoride and mineral profiles of the plaque formed in an in situ plaque-generating device after the exposure to fluoride solutions, using layer-specific analysis [Kato et al., 1997, 2002]. This technique enables us to analyze the distribution of specific materials such as cariogenic bacteria in the dental plaque structure. The aim of this study was to develop a method which could clarify the distribution pattern of cariogenic oral streptococci, *S. mutans* and *S. sobrinus*, throughout the plaque grown on an in situ device placed on the specific tooth site.

Materials and Methods

Plaque Sampling

In situ plaque-generating devices containing plaque receptacles (2 mm in diameter and 0.8–1 mm deep) were made by attaching nylon rings to autoclaved natural enamel slabs [Robinson et al., 1997]. Ten consenting healthy volunteers, 5 males and 5 females, 21–45 years of age, wore these sampling devices to collect plaque from either the upper left or upper right dental arch, using a custom-made dental alloy clasp, as previously reported [Kato et al., 1997]. The subjects were advised to use nonfluoridated toothpaste from at least 1 week before the plaque collection, avoiding rinsing with therapeutic mouthwash. They were asked to form plaque within the devices by abstaining from tooth brushing or by removing the appliances for oral hygiene without toothpaste, after which they were replaced at the same site. After a plaque formation period lasting for 3 days, the devices on the clasps were collected for analysis at least 1 h after any food or drink intake. The DMFS scores were also recorded by oral examination. The experimental design was approved by the Ethics Committee of Aichi-Gakuin University.

Plaque Sample Preparation

The devices, removed from the mouth, were snap-frozen in liquid nitrogen and freeze-dried overnight. They were then impregnated with a mixture of 10% methyl and 90% *n*-butyl methacrylate (Sigma Chemical, St. Louis, Mo., USA). Series of plaque sections parallel to the tooth surface (containing 4 sections of 4 μm thickness and 2 sections of 2 μm thickness; total 20 μm thickness) were repeatedly cut from the outer plaque surface towards the enamel surface, using an ultramicrotome (Ultrotome, LKB, Sweden). Sectioning continued until no sample remained. Each plaque sample was separated into several (8–10) sequential 100-μm-thick specimens consisting of five sets of serial sections (i.e. 20 μm × 5) using this procedure.

Out of the series of plaque sections, 2-μm-thick sections were spread on a glass slide, stained with a 0.05% neutral toluidine blue solution and used to check the presence of plaque. Five series of thicker sections were combined in sequential order and placed in a 0.5-ml sterilized polypropylene tube. Then, chloroform (200 μl) was poured into each tube to dissolve the polymer infiltrated into the specimen. After evaporation, the plaque specimen remained at the bottom of the tube. The preparation of the plaque samples is shown in figure 1.

PCR Analysis

200 μl of the InstaGene Matrix Kit (Bio-Rad Laboratories, Richmond, Calif., USA) was added to each tube. Genomic DNA was extracted from the plaque fraction according to the manufacturer's instructions. The 16S rRNA gene sequences were amplified by PCR with universal primers: 8UA and 1492R [Sato et al., 1997] and *Taq* DNA polymerase (HotStarTaq Master Mix, Qiagen GmbH, Hilden, Germany) according to the manufacturer's instructions. The primer sequences were: 8UA, 5′-AGA GTT TGA TCC TGG CTC AG-3′; and 1492R, 5′-TAC GGG TAC CTT GTT ACG ACT T-3′. PCR amplification was performed in a PCR Thermal Cycler MP (TaKaRa Biomedicals, Ohtsu, Shiga, Japan) programmed for 15 min at 95°C for initial heat activation and 35 cycles of 1 min at 94°C for denaturation, 1 min at 55°C for annealing, and 1.5 min at 72°C for extension, followed by 10 min at 72°C for a final extension. The predicted PCR product with the universal primers was 1,505 bp in length.

Then the PCR products were amplified by the species-specific PCR based on the 16S rRNA gene sequences [Rupf et al., 2001] with *S. mutans*-specific primers sm1 and sm2, and with *S. sobrinus*-specific primers SobF and SobR. The nested primer sequences were as follows: *S. mutans*-forward primer (sm1), 5′-GGT CAG GAA AGT CTG GAG TAA AAG GCT A-3′; *S. mutans*-reverse primer (sm2), 5′-GCG TTA GCT CCG GCA CTA AGC C-3′; *S. sobrinus*-forward primer (SobF), 5′-CGG ACT TGC TCC AGT GTT ACT AA-3′; and

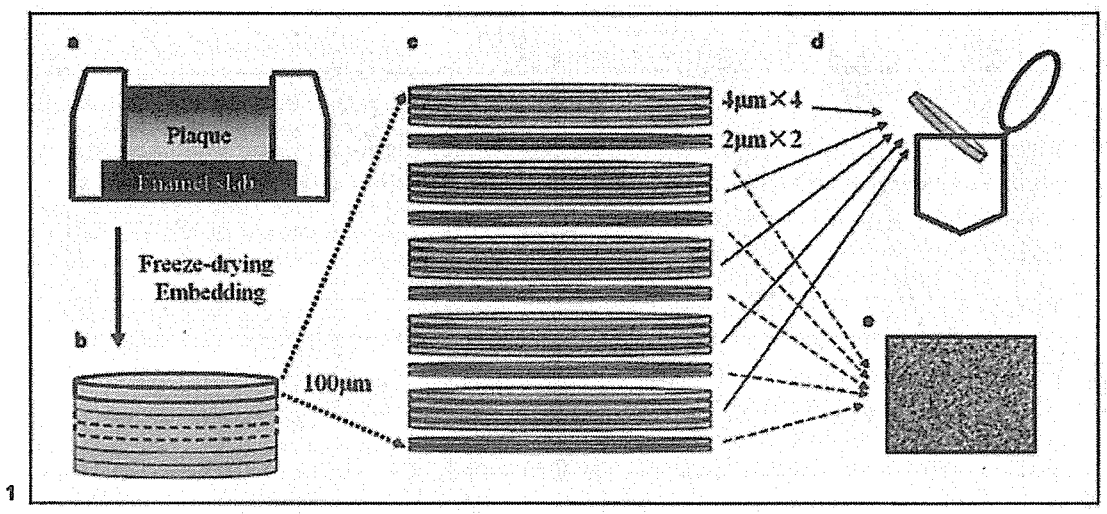

1

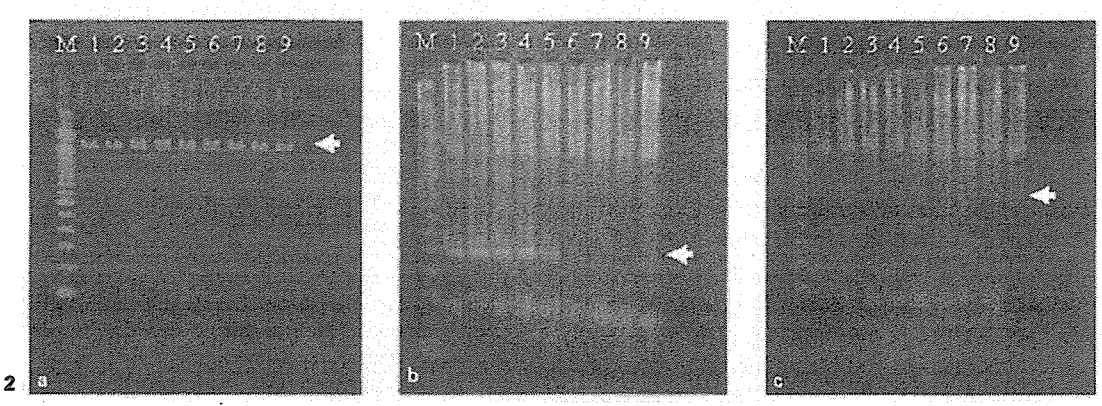

2

Fig. 1. a Plaque in the plaque-generating device. b Arrangement of 100-μm-thick layers in the plaque sample. c Sectioning process for obtaining one layer. d Collection of thicker sections for nested PCR analysis. e Optical observation of stained thinner sections.

Fig. 2. Detection of 16S rRNA gene amplified by PCR with universal primers (a) and the PCR products amplified by *S. mutans*-specific (b) and *S. sobrinus*-specific (c) nested primers. Positive bands are indicated with arrows. A sample taken from subject F was divided into 8 layers. M indicates 100-bp DNA markers. Lanes 1 and 8 are the outermost (1st) and the innermost (8th) layers, respectively. Lane 9 is a blank control without plaque fragments.

S. sobrinus-reverse primer (SobR), 5′-GCC TTT AAC TTC AGA CTT AC-3′. PCR amplification was carried out as previously described. The sizes of the expected PCR products of *S. mutans* and *S. sobrinus* were 282 and 546 bp, respectively.

PCR products were separated on 2% agarose gels using electrophoresis in TBE buffer (100 m*M* Tris, 90 m*M* boric acid, 1 m*M* EDTA, pH 8.4), stained with ethidium bromide and photographed under UV light. A 100-bp DNA ladder (Invitrogen Corp., Carlsbad, Calif., USA) was used as the molecular size marker.

Blank control without any plaque fragments was prepared in order to check the extraction of genomic DNA from the specimen and the presence of contamination. An example of the procedure used on cariogenic bacteria from the gel is shown in figure 2.

Results

S. mutans were detected in the plaque taken from all of the 10 subjects, and *S. sobrinus* in the plaque of 7 of the subjects (table 1). However, both strains were not always detected in every layer of the plaque, although both were found throughout the plaque taken from 1 participant (subject D). These positive layers were also recognized continuously, although the layers containing *S. mutans* were dispersed in the plaque taken from subjects B, G and I. The proportions of layers in which *S. mutans* and *S. so-*

Table 1. Detection patterns of mutans streptococci in layers of 3-day-old plaque taken from 10 subjects

	S. mutans										*S. sobrinus*									
Subject	A	B	C	D	E	F	G	H	I	J	A	B	C	D	E	F	G	H	I	J
DMFS	1	2	4	6	8	10	19	20	22	55	1	2	4	6	8	10	19	20	22	55
Layers																				
1	+	±	+	+	+	+	–	–	+	–	–	–	–	+	+	–	–	–	–	–
2	+	–	+	+	+	+	+	+	+	–	+	–	–	+	+	+	+	+	+	–
3	+	+	+	+	+	+	–	+	+	–	+	–	–	+	+	+	–	+	+	–
4	+	+	+	+	+	+	–	+	+	–	+	–	–	+	+	–	–	+	+	–
5	+	+	+	+	+	+	–	+	+	–	+	–	–	+	+	–	–	+	±	–
6	+	–	–	+	–	+	–	+	±	+	–	–	–	+	±	–	–	+	–	–
7	+	–	–	+	–	–	+	+	–	±	–	–	–	+	–	–	–	–	–	–
8	–	–	–	+	–	–	–	–	+	–	–	–	–	+	–	–	–	–	–	–
9	–	–	n.s.	+	–	n.s.	–	–	±	n.s.	–	–	n.s.	+	–	n.s.	–	–	–	n.s.
10	n.s.	+	n.s.	+	n.s.	n.s.	–	–	–	n.s.	n.s.	–	n.s.	±	n.s.	n.s.	–	–	–	n.s.

The number of plaque layers varied from 8 to 10 with the thickness of individual plaque, layer 1 being the outermost layer, layer 10 the innermost layer. n.s. = No sample available; + = detected; – = not detected; ± = detection difficult to judge.

brinus were detected were 56.5% (52/92) and 31.5% (29/92), respectively.

For the 7 subjects who had both species in their plaque, the distribution pattern of *S. mutans* in the plaque layers was compared to that of *S. sobrinus*. In every layer detected as mutans streptococci-positive, either only *S. mutans* or both species were detected. There were no layers in which *S. sobrinus* was clearly detected alone. Also there was a tendency for mutans streptococci to be frequently detected in the outer to middle layers of plaque, and these bacteria were seldom seen in the inner layers. The distribution pattern of mutans streptococci varied among the subjects, even though the results were obtained only from a small number of samples.

There was no obvious relationship between the pattern and distribution of mutans streptococci and the subjects' DMFS scores.

Discussion

The PCR using universal primers showed a positive band in every layer of dental plaque, indicating the existence of some bacteria throughout the plaque. Oral streptococci are aciduric facultative anaerobes and were therefore expected to be detected equally in both the outer aerobic and the inner anaerobic environments, irrespective of plaque structure. Nevertheless, the distributions of mutans streptococci-positive layers were limited, being seldom found in the inner plaque with the exception of subject D who had fully positive layers. The innermost layer corresponded to the bottom of the thick microbial deposit generated in the artificial stagnation site. It seemed to be difficult for mutans streptococci to survive in such an environment with a limited supply of nutrients such as sugar and with less pH drop. Thus, the levels of bacteria in the deeper layers in our devices might be below the detection limit of our microbiological method, even though it is claimed that this nested PCR could detect 100 and 10 fg DNA of *S. mutans* and *S. sobrinus*, respectively [Sato et al., 2003]. On the other hand, Dibdin and Shellis [1988] suggested that plaque formed in the presence of sucrose promoted porosity of the extracellular matrix. A fully positive pattern for mutans streptococci as seen in subject D's plaque or a dispersed pattern of *S. mutans* as seen in some samples might be the reflection of the subjects' sugar intake under the plaque formation.

The high prevalence rate of mutans streptococci found in various populations [Beighton et al., 1989; Fure and Zickert, 1990; Köhler et al., 1995; Milgrom et al., 2000; Okada et al., 2002] has been well documented, indicating that *S. mutans* was more widespread than *S. sobrinus*. In our depth-specific analysis, every mutans streptococci-positive layer was one in which either only *S. mutans* or both species were detected, suggesting that *S. mutans* has a wider habitat in plaque than *S. sobrinus* has. The results also revealed that mutans streptococci tended to be detected in the outer or middle plaque layers, demonstrating

the different distribution patterns of cariogenic bacteria between the subjects. Milgrom et al. [2000] revealed that *S. mutans* were found more frequently than *S. sobrinus* in the plaque on initial caries lesions as well as on sound enamel. Okada et al. [2002] reported that subjects that harbored both *S. mutans* and *S. sobrinus* had higher caries prevalence. In the present results, however, no obvious relationship was recognized between the distribution patterns of mutans streptococci throughout plaque and the subjects' DMFS scores. This might be due to the microbial difference between natural plaque and plaque formed in the device or due to the F component that accounted for almost all of the DMFS scores.

In the present study, layer-specific samples were prepared from newly formed 3-day-old plaque, with which more than half of the device's receptacles was filled. The plaque sample was formed with an uneven outer surface, tending to be thicker on or near the nylon edge of the device by incomplete filling of the ring. With the progress of sectioning from the plaque-saliva interface, the first layer that contained sections with toluidine blue-stained fragments was regarded as the outermost one. Therefore, the outermost layer might not exactly correspond to the outer plaque surface. However, the surface in a functional sense must correspond to the outer few layers, because the plaque layers that we dealt with were fairly thick. Our results, shown in table 1, demonstrated the effectiveness of this method, suggesting ecological features of mutans streptococci such as a frequent detection in the outer region, a wider habitat of *S. mutans* compared with *S. sobrinus* and so on. Therefore, any influence of this weakness, which stemmed from the unevenness of the outer plaque surface, would be limited to the evaluation of cariogenic bacteria within the plaque from their distribution patterns, so that in general this problem is not serious.

Although several analytical methods [Babaahmady et al., 1998; Milgrom et al., 2000; Rupf et al., 2001] have been used to identify the specific bacteria in plaque, there are only sparse data available concerning the three-dimensional plaque structure. In an attempt to clarify the etiology of periodontal disease, immunofluorescence studies have been carried out to locate the specific pathogens in the periodontal pockets, using sections obtained from biopsy samples of the tissue [Christersson et al., 1987; Noiri et al. 2001]. However, it would be difficult, using this technique, to ensure the location of the bacteria due to disturbances in the process of plaque sampling and preparation followed by staining. Moreover, fluorescence detection under the ordinary light microscope probably has inadequate resolution because of the short duration of the fluorescence. Fluorescence imaging by CLSM has also been applied to examine the heterogeneous structure of the plaque biofilms [Wood et al., 2000] and to clarify bacterial vitality relating to plaque structure [Auschill et al., 2001]. CLSM enabled us to examine the bulk specimens to identify several species by using different fluorochromes. There is, however, a great disparity of thickness between our sample and the thinner plaque for a CLSM observation. In addition, the autofluorescence of enamel may cause less accuracy of location of bacteria near the plaque-enamel interface.

On the other hand, our devices were snap-frozen in liquid nitrogen, lyophilized, then impregnated with methacrylate. Care must be taken to prevent distortion due to uneven drying. Serial sectioning of such an embedded undisturbed plaque sample ensures the validity of our depth-specific analysis of plaque from the outer surface towards the interior. Another advantage of our method is that it would be suitable for quantitative analysis. Although plaque mass or density is different from each layer or individual plaque, this difference is correctable. Plaque volume could be determined by measuring plaque area using image analysis, since section thickness is known. Quantitative differences of cariogenic bacteria have been detected in approximal plaque by an immunofluorescence study [Babaahmady et al., 1998]. It would be interesting to evaluate variations in plaque bacteria at different tooth sites, as well as at comparable sites from different teeth or different individuals. However, it would be difficult to apply the present method at sites on which the devices could not be attached, such as approximal and subgingival spaces.

Our depth-specific assay demonstrated variances in the pattern and distribution of mutans streptococci among our subjects, suggesting that it was important to evaluate their ecology within dental plaque. Further studies are needed to evaluate the bacterial pattern in plaque under various experimental conditions.

Acknowledgments

This work was supported by Grant-in-Aid for Scientific Research (C) No. 14571974 and AGU High-Tech Research Center Project from the Ministry of Education, Culture, Sports, Science and Technology, Japan.

References

Auschill TM, Arweiler NB, Netuschil L, Brecx M, Reich E, Sculean A: Spatial distribution of vital and dead microorganisms in dental biofilms. Arch Oral Biol 2001;46:471–476.

Babaahmady KG, Challacombe SJ, Marsh PD, Newman HN: Ecological study of *Streptococcus mutans*, *Streptococcus sobrinus* and *Lactobacillus* spp. at sub-sites from approximal dental plaque from children. Caries Res 1998;32: 51–58.

Beighton D, Manji F, Baelum V, Fejerskov O, Johnson NW, Wilton JM: Associations between salivary levels of *Streptococcus mutans*, *Streptococcus sobrinus*, lactobacilli, and caries experience in Kenyan adolescents. J Dent Res 1989;68:1242–1246.

Caufield PW, Cutter GR, Dasanayake AP: Initial acquisition of mutans streptococci by infants: Evidence for a discrete window of infectivity. J Dent Res 1993;72:37–45.

Christersson LA, Albini B, Zambon JJ, Wikesjö UM, Genco RJ: Tissue localization of *Actinobacillus actinomycetemcomitans* in human periodontitis. I. Light, immunofluorescence and electron microscopic studies. J Periodontol 1987;58:529–539.

Cury JA, Rebelo MAB, Del Bel Cury AA, Derbyshire MTVC, Tabchoury CPM: Biochemical composition and cariogenicity of dental plaque formed in the presence of sucrose or glucose and fructose. Caries Res 2000;34:491–497.

Dibdin GH, Shellis RP: Physical and biochemical studies of *Streptococcus mutans* sediments suggest new factors linking the cariogenicity of plaque with its extracellular polysaccharide content. J Dent Res 1988;67:890–895.

Fure S, Zickert I: Salivary conditions and cariogenic microorganisms in 55-, 65-, and 75-year-old Swedish individuals. Scand J Dent Res 1990; 98:197–210.

Jensen B, Bratthall D: A new method for the estimation of mutans streptococci in human saliva. J Dent Res 1989;68:468–471.

Kato K, Nakagaki H, Arai K, Pearce EI: The influence of salivary variables on fluoride retention in dental plaque exposed to a mineral-enriching solution. Caries Res 2002;36:58–63.

Kato K, Nakagaki H, Takami Y, Tsuge S, Ando S, Robinson C: A method of determining the distribution of fluoride, calcium and phosphorus in human dental plaque and the effect of a single in vivo fluoride rinse. Arch Oral Biol 1997; 42:521–525.

Köhler B, Andréen I, Jonsson B: The earlier the colonization by mutans streptococci, the higher the caries prevalence at 4 years of age. Oral Microbiol Immunol 1988;3:14–17.

Köhler B, Bjarnason S, Finnbogason SY, Holbrook WP: Mutans streptococci, lactobacilli and caries experience in 12-year-old Icelandic urban children, 1984 and 1991. Community Dent Oral Epidemiol 1995;23:65–68.

Lang NP, Hotz PR, Gusberti FA, Joss A: Longitudinal clinical and microbiological study on the relationship between infection with *Streptococcus mutans* and the development of caries in humans. Oral Microbiol Immunol 1987;2:39–47.

Milgrom P, Riedy CA, Weinstein P, Tanner AC, Manibusan L, Bruss J: Dental caries and its relationship to bacterial infection, hypoplasia, diet, and oral hygiene in 6- to 36-month-old children. Community Dent Oral Epidemiol 2000;28:295–306.

Noiri Y, Li L, Ebisu S: The localization of periodontal-disease-associated bacteria in human periodontal pockets. J Dent Res 2001;80: 1930–1934.

Okada M, Soda Y, Hayashi F, Doi T, Suzuki J, Miura K, Kozai K: PCR detection of *Streptococcus mutans* and *S. sobrinus* in dental plaque samples from Japanese pre-school children. J Med Microbiol 2002;51:443–447.

Pienihäkkinen K, Jokela J: Clinical outcomes of risk-based caries prevention in preschool-aged children. Community Dent Oral Epidemiol 2002;30:143–150.

Ritz HL: Fluorescent antibody staining of *Neisseria*, *Streptococcus* and *Veillonella* in frozen sections of human dental plaque. Arch Oral Biol 1969;14:1073–1083.

Robinson C, Kirkham J, Shore RC, Kusa L, Nakagaki H, Kato K, Natress B: A method for quantitative site-specific study of the biochemistry within dental plaque biofilms formed in vivo. Caries Res 1997;31:194–200.

Roeters FJ, van der Hoeven JS, Burgersdijk RC, Schaeken MJ: Lactobacilli, mutans streptococci and dental caries: A longitudinal study in 2-year-old children up to the age of 5 years. Caries Res 1995;29:272–279.

Rupf S, Merte K, Eschrich K, Stösser L, Kneist S: Peroxidase reaction as a parameter for discrimination of *Streptococcus mutans* and *Streptococcus sobrinus*. Caries Res 2001;35:258–264.

Sato T, Matsuyama J, Kumagai T, Mayanagi G, Yamaura M, Washio J, Takahashi N: Nested PCR for detection of mutans streptococci in dental plaque. Lett Appl Microbiol 2003;37: 66–69.

Sato T, Sato M, Matsuyama J, Hoshino E: PCR-restriction fragment length polymorphism analysis of genes coding for 16S rRNA in *Veillonella* spp. Int J Syst Bacteriol 1997;47:1268–1270.

Wood SR, Kirkham J, Marsh PD, Shore RC, Nattress B, Robinson C: Architecture of intact natural human plaque biofilms studied by confocal laser scanning microscopy. J Dent Res 2000;79:21–27.

Int. J. Oral Maxillofac. Surg. 2004; 33: 584–592
doi:10.1016/j.ijom.2004.01.013, available online at http://www.sciencedirect.com

International Journal of
Oral & Maxillofacial Surgery

Research and Emerging Technologies
Pathology

PTC gene mutations and expression of SHH, PTC, SMO, and GLI-1 in odontogenic keratocysts

K. Ohki[1,2], H. Kumamoto[2], R. Ichinohasama[2], T. Sato[3], N. Takahashi[3], K. Ooya[2]

[1]Department of Oral Medicine and Surgery, Division of Maxillofacial Surgery, Graduate School of Dentistry, Tohoku University, Sendai, Japan; [2]Department of Oral Medicine and Surgery, Division of Oral Pathology, Graduate School of Dentistry, Tohoku University, Sendai, Japan; [3]Department of Oral Biology, Division of Oral Ecology and Biochemistry, Graduate School of Dentistry, Tohoku University, Sendai, Japan

K. Ohki, H. Kumamoto, R. Ichinohasama, T. Sato, N. Takahashi, K. Ooya:PTC gene mutations and expression of SHH, PTC, SMO, and GLI-1 in odontogenic keratocysts. Int. J. Oral Maxillofac. Surg. 2004; 33: 584–592.

Abstract. The *Patched* (*PTC*) gene is responsible for basal cell nevus syndrome (BCNS) accompanied by multiple odontogenic keratocysts (OKCs), and its product plays a role in the Sonic hedgehog (SHH) signaling pathway involving smoothened (SMO) and GLI-1. To clarify the role of SHH signaling in OKCs, the expression of SHH, PTC, SMO, and GLI-1 and mutations of *PTC* were examined in 18 sporadic, 4 BCNS-associated OKCs and 7 control gingivae. SHH, PTC, SMO, and GLI-1 were detected in all OKC and gingiva samples by reverse transcriptase-polymerase chain reaction (RT-PCR). Immunoreactivity for SHH and GLI-1 was markedly higher in epithelial components than in subepithelial cells, while immunoreactivity for PTC and SMO was similar in epithelial components and subepithelial cells in OKCs. The positive rate of PTC and SMO expression in subepithelial cells of OKCs was significantly higher than that in gingivae. The positive rate of GLI-1 expression in subepithelial cells of BCNS-associated OKCs was significantly higher than that in primary OKCs. These results suggest that the SHH signaling might be involved in the pathophysiologic nature of OKCs. While mutations of the *PTC* gene could not be detected in 4 BCNS-associated OKCs by direct DNA sequencing, 3 of 5 primary and 4 of 4 recurrent OKCs had several mutations of this gene. These results suggest that *PTC* mutations are probably related not only to BCNS-associated OKCs but also to sporadic OKCs.

Key words: basal cell nevus syndrome (BCNS); *Patched* (*PTC*); Sonic hedgehog (SHH); Smoothened (SMO); GLI-1; odontogenic keratocyst (OKC).

Accepted for publication 7 January 2004

Available online 18 March 2004

Odontogenic keratocyst (OKC) is the most aggressive odontogenic cyst in the oral cavity[36]. The majority of patients are in their second or third decade of life. Most OKCs arise in the mandible, having a 3-fold higher frequency of OKCs than the maxilla[5,25], while the majority in the mandible was located in the third molar area often with extension into the ascending ramus[37]. Histologically, OKC is characterized by a lining of parakeratotic stratified squamous epithelium and a thin fibrous capsule, which occasionally contain islands of epithelium or separate daughter cysts[6,25]. OKC has a high recurrence rate, estimated to range between 30 and 60%[5,25]. OKC sometimes occurs in association with the basal cell nevus syndrome (BCNS)[5,14]. BCNS, also known as 'Gorlin syndrome' and 'nevoid basal cell carcinoma syndrome,' is a rare autosomal dominant disorder characterized by multiple basal cell carcinomas (BCCs), multiple OKCs, palmar or plantar pits (or both), ectopic calcification, such as calcified flax cerebri, and congenital skeletal anomalies, such as bifid, fused, splayed, or missing ribs[14]. Various low-frequency neoplasms, such as medulloblastomas, meningiomas, fibrosarcomas, ovarian fibromas, and cardiac fibromas, are also associated with BCNS[14].

0901-5027/060584 + 09 $30.00/0

The gene responsible for BCNS has been localized to chromosome 9q22.3-q31 by linkage analysis[11], and the human *Patched* (*PTC*) gene has been isolated from the candidate region[15,20]. The *PTC* gene, bearing strong homology to the *Drosophila* segment polarity gene *patched* (*ptc*), contains 23 exons spanning approximately 34 kbp and encodes a 1447 amino acid protein containing 12 transmembrane-spanning domains and 2 large extracellular loops[19,20,30,38]. Approximately 40% of BCNS cases have germ line mutations of the *PTC* gene. Several *PTC* mutations that are apparently not hereditary have been identified in lesions of BCCs, medulloblastomas, and OKCs[27,34,43,45,46]. In addition, deletions of 9q22.3-q31 were observed on loss of heterozygosity in many neoplasms related to BCNS and in sporadic BCCs and OKCs[12,13,29,34]. PTC product serves as a receptor for the secreted Sonic hedgehog (SHH) protein, and inhibits the signaling pathway by repressing the activity of Smoothened (SMO), another transmembrane membrane protein[1,30,38]. SMO also has a role in reception and transduction of the SHH signal[38]. SMO is responsible for triggering intercellular signaling and the subsequent activation of target genes such as GLI-1. In the absence of SHH, PTC interacts at the membrane with smoothened, rendering it inactive. However, when SHH binds to PTC, the inhibition of SMO signaling is released and downstream genes are transcriptionaly upregulated[44]. GLI-1 is a transcription factor that is thought to form a cytoplasmic complex and mediate SHH signaling from cytoplasm to nucleus[26]. Inherited or sporadic alterations in SHH signaling pathway genes have been implicated in a number of human birth defects, and aberrant activation of the SHH signaling pathway during adult life results in cellular proliferations manifested as cancer[44]. Thus, studying the SHH signaling pathway is essential to understanding the mechanisms of birth defects and cancer and ultimately may help to identify therapeutic targets in diseases involving the SHH signaling pathway[16].

Our previous study examined the proliferative activities, cell-cycle-related factors, and apoptosis-related factors in lining epithelium of solitary and BCNS-associated multiple OKCs. The results suggested that BCNS-associated OKCs might show different characteristics from solitary OKCs[22]. Genetic and immunohistochemical analysis of jaw cysts in *ptc* knockout mice revealed that down-regulation of ptc is associated with formation of the cysts[23]. In the present study, we examined the expression of SHH, PTC, SMO, and GLI-1 at mRNA and protein levels and investigated *PTC* gene mutations in primary, recurrent, and BCNS-associated OKCs. These results of mRNA expression and protein levels were compared with the findings in gingival tissue. On the basis of our findings, we discuss the role of the SHH signaling pathway in OKCs.

Materials and methods

The protocol for the present experiment was reviewed and approved by the Tohoku University Graduate School of Dentistry Research Ethics Committee.

Tissue samples

Specimens were surgically removed from 22 patients with OKC at the Department of Oral and Maxillofacial Surgery, Tohoku University Dental Hospital, and affiliated hospitals. The lesions were divided into several parts. The first part was fixed in 10% buffered formalin for several days and routinely processed for histological diagnosis according to the World Health Organization histological typing of odontogenic tumors[25]. The lesions comprised 13 primary, 5 recurrent, and 4 BCNS-associated OKCs. BCNS was diagnosed according to Gorlin's criteria, including at least two of the following findings: multiple basal cell carcinoma, any odontogenic keratocyst, palmar or plantar pits, ectopic calcification, or a family history of BCNS[9,14]. The second part of each lesion was immediately frozen and stored at −80 °C until RT-PCR analysis and direct DNA sequencing. The third part of each cyst was embedded in Tissue-Tek O.C.T. compound (Sakura Finetechnical, Tokyo, Japan), quick frozen, and stored at −80 °C for immunohistochemical examination. As control, seven normal gingiva samples were obtained at autopsy, performed at Tohoku University Medical Hospital.

RT-PCR

Total RNA from frozen samples (20 mg) of 11 primary OKCs, 3 recurrent OKCs, 4 BCNS-associated OKCs, and 5 normal gingivae was extracted with the use of a RNeasy Mini Kit (Qiagen, Hilden, Germany) according to the recommendations of the manufacturer's protocol. Total RNA (2 μg) was reverse-transcribed with an Omniscript RT Kit (Qiagen) according to the manufacturer's instructions in a 20-μl volume. The complementary DNA (cDNA) (0.05 μg) was used as a template for amplification in a Mastercycler gradient (Eppendorf, Hamburg, Germany) with each primer set[8,15,39,40] as listed in Table 1. PCR was performed on 50 μl of a reaction mixture containing approximately 50 ng

Table 1. RT-PCR primers and antibodies

	Primer			Antibody		
	Sequence (5′-3′)	Annealing temperature (°C)	Product size (bp)	Clonality	Source	Dilution
SHH	F: GAAAG CAGAG AACTC GGTGG R: GGAAA GTGAG GAAGT CGCTG	57	170	Polyclonal (goat)	Santa Cruz Biotechnology, Santa Cruz, CA, USA	1:50
PTC	F: GTGGC TGAGA GCGAA GTTTC R: TTCCA CCCAC AGCTC CTC	60	163	Polyclonal (rabbit)	Santa Cruz Biotechnology	1:50
SMO	F: CTGGT ACGAG GACGT GGAGG R: AGGGT GAAGA GCGTG CAGAG	65	132	Polyclonal (goat)	Santa Cruz Biotechnology	1:50
GLI-1	F: CAGAG AATGG AGCAT CCTCC R: TTCTG GCTCT TCCTG TAGCC	60	413	Polyclonal (goat)	Santa Cruz Biotechnology	1:100
GAPDH	F: GGAGT CAACG GATTT GGT R: GTGAT GGGAT TTCCA TTGAT	62	206			

of template cDNA, 0.5 mol/l of each primer, and 25 µl of HotStarTaq Master Mix (Qiagen), according to the manufacturer's instructions. The conditions for amplification were optimized for primer pairs as follows: heat starting at 95 °C for 15 min; 45 cycles of denaturation at 94 °C for 30 s, annealing at 63 °C (for PTC and SHH), 65 °C (for SMO), 60 °C (for GLI-1), and 62 °C (for glyceraldehyde-3-phosphate dehydrogenase (GAPDH)) for 30 s, and elongation at 72 °C for 1 min; and final extension at 72 °C for 10 min. The RT-PCR amplified products were applied to 2% agarose gel, electrophoresed in 1 × TBE at 100 V for 30 min, stained with ethidium bromide, and visualized under ultraviolet (UV) light.

Immunohistochemical examination of SHH, PTC, SMO, and GLI-1 proteins

Serial frozen sections were cut at a thickness of 5 µm in a cryostat CM3000 (Leica, Bensheim, Germany), placed on glass slides, air-dried for 30 s at room temperature (22 °C), and fixed in acetone for 10 min at 4 °C. The slides were then rinsed for 15 min in 0.01 M phosphate buffer solution (PBS). After treatment with normal rabbit serum for 15 min to block non-specific binding, the sections were incubated with primary antibodies at 4 °C overnight. The applied antibodies are listed in Table 1. The standard streptavidin–biotin–peroxidase complex method was performed to bind the primary antibodies with use of a Histofine SAB-PO kit (Nichirei, Tokyo, Japan). Reaction products were visualized by immersing the sections for 1–5 min in 0.03% 3,3′-diaminobenzidine (DAB) solution containing 2 mM hydrogen peroxide. Nuclei were lightly counterstained with 1% methyl green. For control studies of the antibodies, the serial sections were treated with PBS and normal goat and rabbit IgG instead of the primary antibodies and were confirmed to be unstained.

Evaluation of immunostaining and statistical analysis

Immunohistochemical reactivity for SHH, PTC, SMO, and GLI-1 was evaluated and classified into three groups: (−) negative, (+) positive (less than 50% of epithelial cells or subepithelial fibroblasts stained), and (++) strongly positive (more than 50% of epithelial cells or subepithelial fibroblasts stained). The statistical significance of differences in the percentages of cases with different reactivity levels for SHH, PTC, SMO, and GLI-1 was analyzed by Pearson's chi-square test. *P* values less than 0.05 were considered to indicate statistical significance.

DNA extraction and direct DNA sequencing

Genomic DNA from frozen samples (25 mg) of 5 primary OKCs, 4 recurrent OKCs, and 4 BCNS-associated OKCs was extracted with a QIAamp DNA Mini Kit (Qiagen) according to the recommendations of the manufacturer's protocol. Each of the 20 exons (exon 2–19, 21, 22) comprising the *PTC* gene were separately amplified in a Mastercycler gradient (Eppendorf) with use of the oligonucleotide primers as described previously[15,28] (Table 2). PCR was performed on 50 µl of a reaction mixture containing approximately 50 ng of template DNA, 0.5 µmol/l of each primer, and 25 µl of HotStarTaq Master Mix (Qiagen) according to the manufacturer's instructions. The conditions for amplification were optimized for primer pairs as follows: heat starting at 95 °C for 15 min; 45 cycles of denaturation at 94 °C for 30 s, annealing at 57–60 °C for 10 s, and elongation at 72 °C for 1 min; and final extension at 72 °C for

Table 2. Primers for DNA sequencing

Exon	Sequence (5′-3′)	Annealing temperature (°C)	Exon size (bp)
2	F: GTGGC TGAGA GCGAA GTTTC	57	193
	R: TTCCA CCCAC AGCTC CTC		
3	F: CTATT GTGTA TCCAA TGGCA GG	60	200
	R: ATTAG TAGGT GGACG CGGC		
4	F: GAGAA ATTTT TGTCT CTGCT TTTCA	57	60
	R: CCTGA TCCAT GTAAC CTGTT TC		
5	F: GCAAA AATTT CTCAG GAACA CC	57	92
	R: TGGAA CAAAC AATGA TAAGC AA		
6	F: CCTAC AAGGT GGATG CAGTG	57	199
	R: TTTGC TCTCC ACCCT TCTGA		
7	F: GTGAC CTGCC TACTA ATTCC C	60	122
	R: GGCTA GCGAG GATAA CGGTT TA		
8	F: GAGGC AGTGG AAACT GCTTC	57	148
	R: TTGCA TAACC AGCGA GTCTG		
9, 10	F: GTGCT GTCGA GGCTT GTG	60	Exon 9: 132,
	R: ACGGA CAGCA GATAA ATGGC		exon 10: 157
11	F: GTGTT AGGTG CTGGT GGCA	60	98
	R: CTTAG GAACA GAGGA AGCTG		
12	F: GACCA TGTCC AGTGC AGCTC	60	245
	R: CGTTC AGGAT CACCA CAGCC		
	F: AGTCC CTGAT TGGGC GGAG	60	
	R: CCATT CTGCA CCCAA TCAAA AG		
13	F: GGCCT ACACC GACAC ACAC	60	403
	R: TTTTT TTGAA GACAG GAAGA GCC		
	F: GTCAG CAGAC TGATT CAGGT	57	
	R: AAGAT GAGAG TGTCC ACTTC G		
14	F: GACAG CTTCT CTTTG TCCAG	60	310
	R: ACGCA AAAGA CCGAA AGGAC GA		
15	F: AGGGT CCTTC TGGCT GCGAG	60	143
	R: TCAGT GCCCA GCAGC TGGAG TA		
16	F: AACCC CATTC TCAAA GGCCT CTGTT C	60	184
	R: CACCT CTGTA AGTTC CCAGA CCTCC		
17	F: AACTG TGATG CTCTT CTACC CTGG	60	281
	R: AAACT TCCCG GCTGC AGAAA GA		
18	F: TTTGA TCTGA ACCGA GGACA CC	60	138
	R: CAAAC AGAGC CAGAG GAAAT GG		
19	F: TAGGA CAGAG CTGAG CATTT ACC	57	143
	R: TACCT GACAA TGAAG TCG		
21	F: AACAG AGGCC CCTGA AAAAT	60	255
	R: GATCA CTTGG TGGGC AGG		
22	F: TCTAA CCCAC CCTCA CCCTT	57	538
	R: ATTGT TAGGG CCAGA ATGCC		
	F: AGAAA AGGCT TGTGG CCAC	60	
	R: TCACC CTCAG TTGGA GCTG		

10 min. Direct sequencing of the *PTC* gene exons was carried out by means of the above mentioned PCR primers, the PCR products purified on the GFX PCR DNA and a Gel Band Purification Kit (Amersham Biosciences, Little Chalfont, UK), and a Thermo Sequenase Cy5 Dye Terminator Sequencing Kit (Amersham Biosciences) according to the manufacturers' instructions. The sequencing reactions were for 45 cycles of 96 °C for 30 s, 60 °C for 10 s, and 72 °C for 60 s in a Mastercycler gradient (Eppendorf). Sequencing products were separated on denaturing 7% polyacrylamide gel (ReproGel Long Read; Amersham Biosciences), using an automated laser fluorescence sequencer (ALF express II DNA Sequencer; Amersham Biosciences). Sequencing data were analyzed with the use of an ALFwin Sequence Analyser Ver. 2.1 (Amersham Biosciences).

Genbank accession data

Nucleotide and amino-acid residue numbering is based on Genbank sequence U59464.

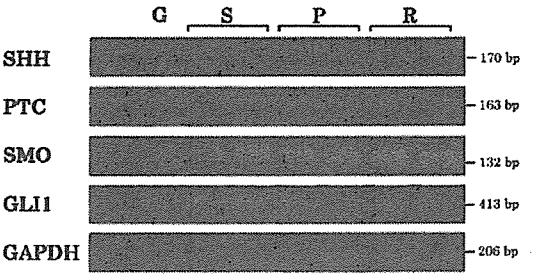

Fig. 1. SHH, PTC, SMO, and GLI-1 mRNA expression in odontogenic keratocysts (OKCs) and normal gingiva. (G: gingiva, S: BCNS-associated OKC, P: primary OKC, R: recurrent OKC). Reverse transcriptase-polymerase chain reaction (RT-PCR) products for SHH (170 bp), PTC (163 bp), SMO (132 bp), and GLI-1 (413 bp) were detected in all gingiva and OKC samples.

Results

Expression of SHH, PTC, SMO, and GLI-1 mRNA

To investigate the distribution patterns of SHH, PTC, SMO, and GLI-1 mRNA in OKCs, we examined 18 OKCs of different clinical characterization (11 primary OKCs, 3 recurrent OKCs, and 4 BCNS-associated OKCs) as well as 5 normal gingivae by RT-PCR analysis. RT-PCR products for SHH (170 bp), PTC (163 bp), SMO (132 bp), and GLI-1 (413 bp) were detected in all OKC and gingiva samples. Fig. 1 shows examples of SHH, PTC, SMO, and GLI-1 mRNA expression in OKCs and normal gingiva.

Immunoreactivity for SHH, PTC, SMO, and GLI-1

The results for immunohistochemical expression of SHH, PTC, SMO, and GLI-1 proteins are shown in Table 3. Fig. 2A–D shows typical staining of

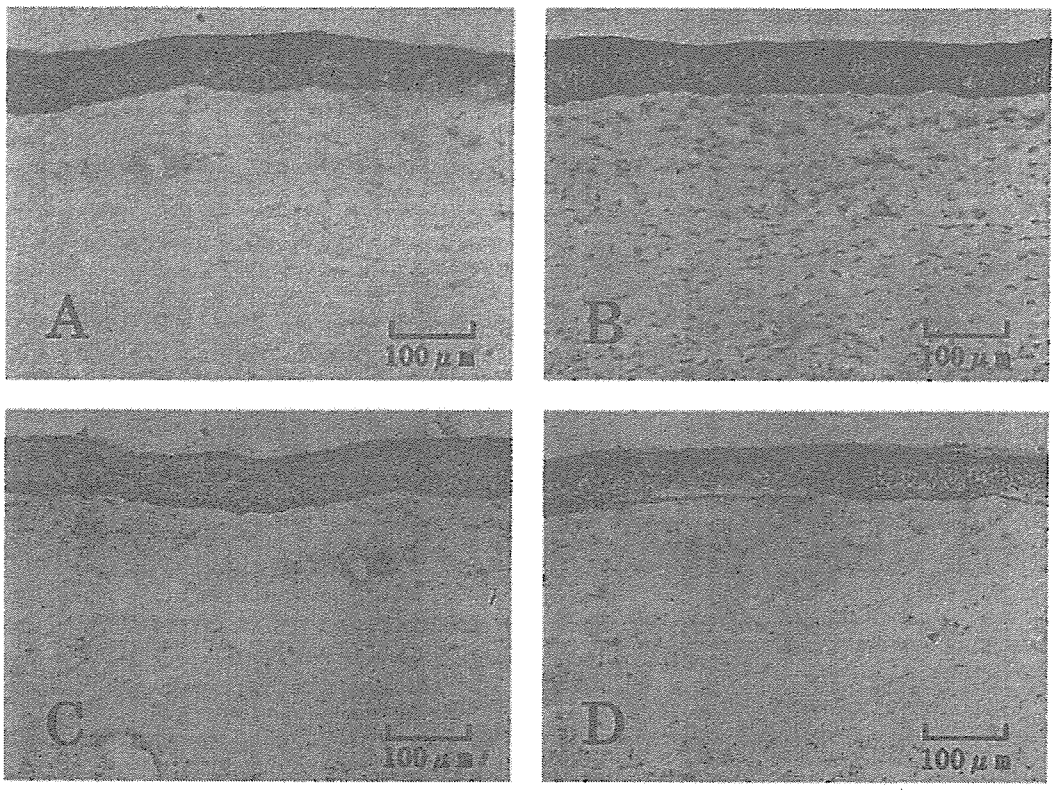

Fig. 2. Immunohistochemical expression of SHH (A), PTC (B), SMO (C), and GLI-1 (D) in odontogenic keratocyst. SHH, PTC, SMO, and GLI-1 were detected in the cytoplasm of basal to superficial epithelial cells. The positive rate of PTC expression in the cytoplasm of subepithelial fibroblasts was higher then that of SHH, SMO, and GLI-1.

Table 3. Immunohistochemical expression of SHH, PTC, SMO, and GLI-1 in gingivae and odontogenic keratocysts

			SHH			PTC			SMO			GLI-1		
			-	+	++	-	+	++	-	+	++	-	+	++
Gingiva (n = 7)		Covering epithelium	0 (0%)	1 (14%)	6 (86%)	0 (0%)	1 (14%)	6 (86%)	0 (0%)	4 (57%)	3 (43%)	0 (0%)	5 (71%)	2 (29%)
		Connective tissue	4 (57%)	3 (43%)	0 (0%)	3 (43%)	4 (57%)	0 (0%)	2 (29%)	5 (71%)	0 (0%)	7 (100%)	0 (0%)	0 (0%)
OKC	Total (n = 22)	Lining epithelium	0 (0%)	0 (0%)	22 (100%)	0 (0%)	2 (9%)	20 (91%)	0 (0%)	4 (18%)	18 (82%)	0 (0%)	6 (27%)	16 (73%)
		Connective tissue	4 (18%)	18 (82%)	0 (0%)	0 (0%)	4 (18%)	18 (82%)	0 (0%)	14 (64%)	8 (36%)	12 (55%)	8 (36%)	2 (9%)
	Primary-OKC (n = 13)	Lining epithelium	0 (0%)	0 (0%)	13 (100%)	0 (0%)	1 (8%)	12 (92%)	0 (0%)	2 (15%)	11 (85%)	0 (0%)	5 (38%)	8 (62%)
		Connective tissue	2 (15%)	11 (85%)	0 (0%)	0 (0%)	2 (15%)	11 (85%)	0 (0%)	8 (62%)	5 (38%)	10 (77%)	3 (23%)	0 (0%)
	Recurrent-OKC (n = 5)	Lining epithelium	0 (0%)	0 (0%)	5 (100%)	0 (0%)	1 (20%)	4 (80%)	0 (0%)	2 (40%)	3 (60%)	0 (0%)	0 (0%)	5 (100%)
		Connective tissue	2 (40%)	3 (60%)	0 (0%)	0 (0%)	1 (20%)	4 (80%)	0 (0%)	4 (80%)	1 (20%)	2 (40%)	2 (40%)	1 (20%)
	BCNS-OKC (n = 4)	Lining epithelium	0 (0%)	0 (0%)	4 (100%)	0 (0%)	0 (0%)	4 (100%)	0 (0%)	0 (0%)	4 (100%)	0 (0%)	1 (25%)	3 (75%)
		Connective tissue	0 (0%)	4 (100%)	0 (0%)	0 (0%)	1 (25%)	3 (75%)	0 (0%)	2 (50%)	2 (50%)	0 (0%)	3 (75%)	1 (25%)

Immunohistochemical expression: (−) negative, (+) positive, (++) strongly positive. Statistical significance: $^{*}P < 0.05$, $^{**}P < 0.01$, $^{***}P < 0.001$.

Table 4. PTC gene mutations in odontogenic keratocysts (OKCs)

Patient	Diagnosis	Mutations		
		Exon	Nucleotide change	Amino acid change
1	Primary OKC	12	C1686T (silent mutation)	Ala562Ala
2	Primary OKC	22	G3840T (silent mutation)	Ser1280Ser
		22	G3852T (missense mutation)	Gln1284His
		22	C3859T (missense mutation)	His1287Asn
		22	C3905A (missense mutation)	Ser1302His
3	Primary OKC	22	G3852T (missense mutation)	Gln1284His
		22	C3875T (missense mutation)	Ser1292Phe
		22	C3905A (missense mutation)	Pro1302His
4	Primary OKC	No mutation		
5	Primary OKC	No mutation		
6	Recurrent OKC	4	635insG (frameshift mutation)	
		4	638insG (frameshift mutation)	
7	Recurrent OKC	10	1371delG (frameshift mutation)	
		22	T3944C (missense mutation)	Leu1315Pro
8	Recurrent OKC	10	1371delG (frameshift mutation)	
9	Recurrent OKC	10	1371delG (frameshift mutation)	
		21	3641delC (frameshift mutation)	
		21	3661insC (frameshift mutation)	
		21	C3728G (missense mutation)	Ala1243Gly
10	BCNS	No mutation		
11	BCNS	No mutation		
12	BCNS	No mutation		
13	BCNS	No mutation		

SHH, PTC, SMO, and GLI-1 proteins in one OKC. SHH, PTC, SMO, and GLI-1 were detected in the cytoplasm of basal to superficial epithelial cells and some subepithelial fibroblasts in both normal gingivae and OKCs. The positive rate of PTC expression in the cytoplasm of subepithelial fibroblasts was higher then that of SHH, SMO, and GLI-1 in OKCs. There was no distinct difference in SHH reactivity between gingivae and OKCs, or among primary, recurrent, and BCNS-associated OKCs. The positive rate of PTC expression in subepithelial tissues of gingivae was significant lower then that of total ($P < 0.001$), primary ($P < 0.01$), recurrent ($P < 0.05$), and BCNS-associated OKCs ($P < 0.05$). The positive rate of SMO expression in subepithelial fibrous connective tissues of OKCs was significantly higher than that in normal gingivae ($P < 0.05$). The positive rate of GLI-1 expression in the subepithelial fibrous connective tissues of BCNS-associated OKCs was significantly higher than that in normal gingivae ($P < 0.05$), and subepithelial GLI-1 expression differed significantly between primary and BCNS-associated OKCs ($P < 0.01$).

Mutations of the *PTC* gene

PTC gene mutations were examined in 5 primary, 4 recurrent, and 4 BCNS-associated OKCs by direct DNA sequencing. Mutations in the coding region of the *PTC* gene were found in 3 primary and 4 recurrent OKCs, whereas no mutation was found in 2 primary and 4 BCNS-associated OKCs (Table 4). Each mutation was confirmed by reverse sequencing. These putative disease-associated mutations were distributed throughout the gene. Eight of the 13 sequence alterations were single nucleotide changes (Fig. 3A), resulting in 6 missense mutations and 2 silent mutations. Six missense mutations were detected in exons 21 and 22, containing 2 C → T and 1 T → C transition, and 1 G → T, 1 C → A, and 1 C → G transversion. We also detected a C → T transition at nucleotide 1686 in exon 12 and a G → T transversion at nucleotide 3840 in exon 22, resulting in silent mutation. Five frameshift mutations were detected (Fig. 3B and C). These single nucleotide deletions or insertions, consisting of G insertion in exon 4, C insertion in exon 21, G deletion in exon 10, and C deletion in exon 21, resulted in the induction of premature stop codons at several bp downstream of the mutation sites. Locations of these mutations on PTC protein are summarized in Fig. 4. In addition to these disease-associated mutations, several variants were designated "polymorphism" on the basis of their presence in unaffected individuals or the finding that the underlying sequence changes did not alter the encoded amino acids.

Discussion

The SHH signaling pathway plays an important role in mammalian embryonic development of structures such as the neural tube, axial skeleton, limbs, lungs, skin, and hair follicles[2,7,17,31,35]. Expression of genes involved in the SHH signaling pathway has been confirmed temporally and spatially during early tooth development, suggesting a role in early tooth germ initiation and subsequent epithelial–mesenchymal interactions. SHH expression was localized to the epithelial thickenings at epithelial thickening stage of tooth development. SHH transcripts were found to be restricted to cells that will form the enamel knot. At the early bud stage, the localized expression of SHH was intensified. By the cap stage, the enamel knot has fully formed and SHH expression clearly marks this structure. PTC and GLI-1 expressions were restricted to the mesenchyme underlying the tooth thickening. At the early bud stage, PTC and GLI-1 were expressed uniformly in the odontogenic epithelium such as dental papilla and dental epithelium, and mesenchyme. At the cap stage of tooth development, PTC and GLI-1 were expressed in a region of the tooth germ that appeared to surround the area of the enamel knot that was marked by SHH expression. SMO was found to be ubiquitously expressed throughout tooth development. With the passage of stage, the expression of SMO was slightly more specific, being more strongly expressed in the epithelial component, but absent from the enamel knot. These features suggest that SHH signaling is involved in both lateral (epithelial-mesenchymal) and planar (epithelial-epithelial) pathways during tooth development[17]. PTC, SMO, and GLI-1 mRNA is up-regulated in BCCs, although tumor-adjacent epidermis shows low expression of these molecules[33,40]. In our previous study, normal gingival tissues were positive for ptc, shh, and smo proteins in *ptc* knockout mice[23]. In the present study, SHH, PTC, SMO, and GLI-1 were detected in all normal gingivae at both mRNA and protein levels, suggesting that gingival tissue might be affected by these molecules.

SHH signaling is emerging as one of the most important regulators of oncogenic transformation[16]. The *PTC* gene

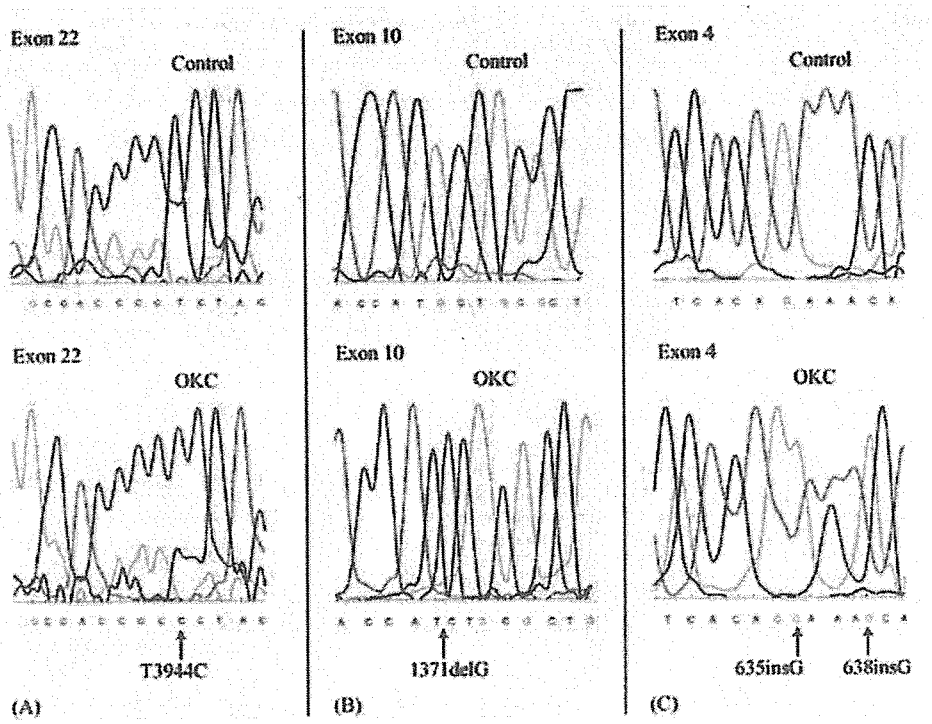

Fig. 3. PTC gene mutations in odontogenic keratocysts (OKCs). (A) Direct DNA sequencing of exon 22 (upper: control, lower: OKC) T to C transitional change at nucleotide 3944, that resulted in leucine to proline substitution at codon 1315. (B) Direct DNA sequencing of exon 10 (upper: control, lower: OKC). A single nucleotide of G was deleted at position 1371, which was expected to result in a stop codon after a run of 33 novel amino acids downstream. (C) Direct DNA sequencing of exon 4 (upper: control, lower: OKC). A single nucleotide of G was inserted at position 635 and 638, which was expected to result in a stop codon after a run of seven novel amino acids downstream.

functions as a tumor suppressor, and *SHH*, *SMO*, and *GLI-1* mutants have been shown to function as oncogenes[8,10,38,46]. Mutational inactivation of *PTC* leads to overexpression of the mutant transcript owing to failure of a negative feedback mechanism[13,41]. Expression studies with *in situ* hybridization and RT-PCR have shown PTC overexpression in BCCs as compared with normal skin[32,41]. Previous studies have demonstrated that SMO is also overexpressed in BCC, whereas SHH is expressed in only some BCCs[21,40]. In the present study, SHH, PTC, SMO, and GLI-1 were detected at mRNA and protein levels in all OKCs. The expression of SHH and GLI-1 was more marked in lining epithelium than in subepithelial cells, while PTC and SMO were similarly expressed in both epithelial and subepithelial cells. These features suggest that SHH signaling is transmitted via epithelial-subepithelial interactions in the cyst walls of OKCs. Our previous study revealed that ptc expression was decreased in lining epithelium of mandibular cysts in *ptc* knockout mice[23]. In the present study, expression of PTC, SMO, and GLI-1 in subepithelial cells was greater in OKCs than in normal gingiva. These findings suggest that OKCs show different characteristics from normal gingival tissues with respect to SHH signaling, and such differences might be involved in the formation of OKCs. Our previous study clarified differences in proliferative activity and apoptotic factors between sporadic and BCNS-associated OKCs[22]. In the present study, GLI-1 expression in subepithelial fibroblasts was slightly higher in BCNS-associated OKCs than in sporadic OKCs. These results suggest that the characteristics of SHH signaling differ between BCNS-associated OKCs and sporadic OKCs.

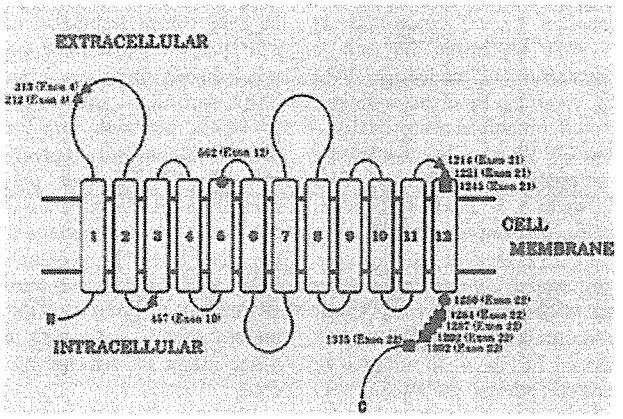

Fig. 4. Location of mutations on PTC protein. (▲: frameshift mutation, ■: missense mutation, ●: silent mutation).

PTC gene mutations are found not only in BCNS but also in sporadic tumors, such as BCC, trichoepithelioma, and medulloblastoma[34,42,45]. Between 20 and 30% of sporadic BCCs show somatic *PTC* mutations, and 68% show

loss of heterozygosity (LOH) on chromosome 9q, the PTC locus[11]. *PTC* mutations and LOH at the PTC locus have been identified in OKCs arising in BCNS and in sporadic OKCs[27,29,47]. In the present study, we identified 13 mutations of the *PTC* gene in three primary OKCs and four recurrent OKCs. These findings suggest that abnormality of the *PTC* gene is essential for the development of OKCs. Generally, exogenous mutagens can cause specific hot spots of somatic mutations in human cancers: for example, the oncogene of *K-RAS* and the tumor suppressor gene of *TP53*[4,18]. Previous studies have shown that *PTC* mutations are dispersed throughout the entire coding sequence of the gene without any apparent hot spots in BCNS-associated lesions[15,20,43,46]. In the present study, mutations of the *PTC* gene were also distributed in a variety of exons. PTC protein possesses several major domains, including the large extracellular loops that interact with SHH ligand and the large C-terminal intracellular domain that may interact with the intracellular protein of SMO protein[3,13,24]. In the present study, most *PTC* mutations of OKCs were detected in the first large extracellular loop or the large C-terminal intracellular domain, suggesting that these mutations inhibit SHH signaling in OKCs. Homozygous *ptc* knockout mice ($ptc^{-/-}$ mice) die in utero during early organogenesis, while $ptc^{+/-}$ mice show a number of developmental abnormalities and a high incidence of tumors, similar to human BCNS[23]. We detected no alteration of the *PTC* gene in BCNS-associated OKCs. These results suggest that the BCNS with germline mutations might cause chromosomal deletion and express another stable allele in OKC tissues.

References

1. Alcedo J, Noll M. Hedgehog and its patched-smoothened receptor complex: a novel signaling mechanism at the cell surface. Biol Chem 1997: **378**: 583–590.
2. Bellusci S, Furuta Y, Rush MG, Henderson R, Winnier G, Hogan BL. Involvement of Sonic hedgehog (Shh) in mouse embryonic lung growth and morphogenesis. Development 1997: **124**: 53–63.
3. Bodak N, Queille S, Avril MF, Bouadjar B, Drougard C, Sarasin A, Daya-Grosjean L. High levels of patched gene mutations in basal-cell carcinomas from patients with xeroderma pigmentosum. Proc Natl Acad Sci USA 1999: **96**: 5117–5122.
4. Bos JL. ras oncogenes in human cancer: a review. Cancer Res 1989: **49**: 4682–4689.
5. Brannon RB. The odontogenic keratocyst. A clinicopathologic study of 312 cases. Part I. Clinical features. Oral Surg Oral Med Oral Pathol 1976: **42**: 54–72.
6. Brannon RB. The odontogenic keratocyst. A clinicopathologic study of 312 cases. Part II. Histologic features. Oral Surg Oral Med Oral Pathol 1977: **43**: 233–255.
7. Chiang C, Swan RZ, Grachtchouk M, Bolinger M, Litingtung Y, Robertson EK, Cooper MK, Gaffield W, Westphal H, Beachy PA, Dlugosz AA. Essential role for Sonic hedgehog during hair follicle morphogenesis. Dev Biol 1999: **205**: 1–9.
8. Dahmane N, Lee J, Robins P, Heller P, Ruiz I, Altaba A. Activation of the transcription factor Gli1 and the Sonic hedgehog signaling pathway in skin tumours. Nature 1997: **389**: 876–881.
9. Evans DG, Ladusans EJ, Rimmer S, Burnell LD, Thakker N, Farndon PA. Complications of the naevoid basal cell carcinoma syndrome: results of a population based study. J Med Genet 1993: **30**: 460–464.
10. Fan H, Oro AE, Scott MP, Khavari PA. Induction of basal cell carcinoma features in transgenic human skin expressing Sonic hedgehog. Nat Med 1997: **3**: 788–792.
11. Gailani MR, Bale SJ, Leffell DJ, DiGiovanna JJ, Peck GL, Poliak S, Drum MA, Pastakia B, McBride OW, Kase R, Greene M, Mulvihill JJ, Bale AE. Developmental defects in Gorlin syndrome related to a putative tumor suppressor gene on chromosome 9. Cell 1992: **69**: 111–117.
12. Gailani MR, Leffell DJ, Ziegler A, Gross EG, Brash DE, Bale AE. Relationship between sunlight exposure and a key genetic alteration in basal cell carcinoma. J Natl Cancer Inst 1996: **88**: 349–354.
13. Gailani MR, Stahle-Backdahl M, Leffell DJ, Glynn M, Zaphiropoulos PG, Pressman C, Unden AB, Dean M, Brash DE, Bale AE, Toftgard R. The role of the human homologue of *Drosophila* patched in sporadic basal cell carcinomas. Nat Genet 1996: **14**: 78–81.
14. Gorlin RJ. Nevoid basal-cell carcinoma syndrome. Medicine 1987: **66**: 98–113.
15. Hahn H, Wicking C, Zaphiropoulos PG, Gailani MR, Shanley S, Chidambaram A, Vorechovsky I, Holmberg E, Unden AB, Gillies S, Negus K, Smyth I, Pressman C, Leffell DJ, Gerrard B, Goldstein AM, Dean M, Toftgard R, Chenevix-Trench G, Wainwright B, Bale AE. Mutations of the human homolog of *Drosophila* patched in the nevoid basal cell carcinoma syndrome. Cell 1996: **85**: 841–851.
16. Hahn H, Wojnowski L, Miller G, Zimmer A. The patched signaling pathway in tumorigenesis and development: lessons from animal models. J Mol Med 1999: **77**: 459–468.
17. Hardcastle Z, Mo R, Hui CC, Sharpe PT. The Shh signalling pathway in tooth development: defects in Gli2 and Gli3 mutants. Development 1998: **125**: 2803–2811.
18. Hollstein M, Shomer B, Greenblatt M, Soussi T, Hovig E, Montesano R, Harris CC. Somatic point mutations in the p53 gene of human tumors and cell lines: updated compilation. Nucleic Acids Res 1996: **24**: 141–146.
19. Hooper JE, Scott MP. The *Drosophila* patched gene encodes a putative membrane protein required for segmental patterning. Cell 1989: **59**: 751–765.
20. Johnson RL, Rothman AL, Xie J, Goodrich LV, Bare JW, Bonifas JM, Quinn AG, Myers RM, Cox DR, Epstein Jr EH, Scott MP. Human homolog of patched, a candidate gene for the basal cell nevus syndrome. Science 1996: **272**: 1668–1671.
21. Kallassy M, Toftgard R, Ueda M, Nakazawa K, Vorechovsky I, Yamasaki H, Nakazawa H. Patched (ptch)-associated preferential expression of smoothened (smoh) in human basal cell carcinoma of the skin. Cancer Res 1997: **57**: 4731–4735.
22. Kimi K, Kumamoto H, Ooya K, Motegi K. Immunohistochemical analysis of cell-cycle- and apoptosis-related factors in lining epithelium of odontogenic keratocysts. J Oral Pathol Med 2001: **30**: 434–442.
23. Kimi K, Ohki K, Kumamoto H, Kondo M, Taniguchi Y, Tanigami A, Ooya K. Immunohistochemical and genetic analysis of mandibular cysts in heterozygous *ptc* knockout mice. J Oral Pathol Med 2003: **32**: 108–113.
24. Koebernick K, Hollemann T, Pieler T. Molecular cloning and expression analysis of the hedgehog receptors XPtc1 and XSmo in *Xenopus laevis*. Mech Dev 2001: **100**: 303–308.
25. Kramer IRH, Pindborg JJ, Shear M. WHO Histological Typing of Odontogenic Tumours. Berlin: Springer-Verlag 1992: 35–36.
26. Lee J, Platt KA, Censullo P, Ruiz I, Altaba A. Gli1 is a target of Sonic hedgehog that induces ventral neural tube development. Development 1997: **124**: 2537–2552.
27. Lench NJ, High AS, Markham AF, Hume WJ, Robinson PA. Investigation of chromosome 9q22.3-q31 DNA marker loss in odontogenic keratocysts. Eur J Cancer B Oral Oncol 1996: **32**: 202–206.
28. Lench NJ, Telford EA, High AS, Markham AF, Wicking C, Wainwright BJ. Characterisation of human patched germ line mutations in naevoid basal cell carcinoma syndrome. Hum Genet 1997: **100**: 497–502.

29. Levanat S, Gorlin RJ, Fallet S, Johnson DR, Fantasia JE, Bale AE. A two-hit model for developmental defects in Gorlin syndrome. Nat Genet 1996: **12**: 85–87.
30. Marigo V, Davey RA, Zuo Y, Cunningham JM, Tabin CJ. Biochemical evidence that patched is the hedgehog receptor. Nature 1996: **384**: 176–179.
31. Marigo V, Tabin CJ. Regulation of patched by Sonic hedgehog in the developing neural tube. Proc Natl Acad Sci USA 1996: **93**: 9346–9351.
32. Nagano T, Bito T, Kallassy M, Nakazawa H, Ichihashi M, Ueda M. Overexpression of the human homologue of *Drosophila* patched (PTCH) in skin tumours: specificity for basal cell carcinoma. Br J Dermatol 1999: **140**: 287–290.
33. Oro AE, Higgins KM, Hu Z, Bonifas JM, Epstein Jr EH, Scott MP. Basal cell carcinomas in mice overexpressing Sonic hedgehog. Science 1997: **276**: 817–821.
34. Raffel C, Jenkins RB, Frederick L, Hebrink D, Alderete B, Fults DW, James CD. Sporadic medulloblastomas contain PTCH mutations. Cancer Res 1997: **57**: 842–845.
35. Riddle RD, Johnson RL, Laufer E, Tabin C. Sonic hedgehog mediates the polarizing activity of the ZPA. Cell 1993: **75**: 1401–1416.
36. Shear M. The aggressive nature of the odontogenic keratocyst: is it a benign cystic neoplasm? Part 1. Clinical and early experimental evidence of aggressive behaviour. Oral Oncol 2002: **38**: 219–226.
37. Stoelinga PJ. Long-term follow-up on keratocysts treated according to a defined protocol. Int J Oral Maxillofac Surg 2001: **30**: 14–25.
38. Stone DM, Hynes M, Armanini M, Swanson TA, Gu Q, Johnson RL, Scott MP, Pennica D, Goddard A, Phillips H, Noll M, Hooper JE, De Sauvage F, Rosenthal A. The tumour-suppressor gene patched encodes a candidate receptor for Sonic hedgehog. Nature 1996: **384**: 129–134.
39. Tojo M, Kiyosawa H, Iwatsuki K, Kaneko F. Expression of a Sonic, hedgehog signal transducer hedgehog-interacting protein, by human basal cell carcinoma. Br J Dermatol 2002: **146**: 69–73.
40. Tojo M, Mori T, Kiyosawa H, Honma Y, Tanno Y, Kanazawa KY, Yokoya S, Kaneko F, Wanaka A. Expression of Sonic hedgehog signal transducers, patched and smoothened, in human basal cell carcinoma. Pathol Int 1999: **49**: 687–694.
41. Unden AB, Zaphiropoulos PG, Bruce K, Toftgard R, Stahle-Backdahl M. Human patched (PTCH) mRNA is overexpressed consistently in tumor cells of both familial and sporadic basal cell carcinoma. Cancer Res 1997: **57**: 2336–2340.
42. Vorechovsky I, Unden AB, Sandstedt B, Toftgard R, Stahle-Backdahl M. Trichoepitheliomas contain somatic mutations in the overexpressed PTCH gene: support for a gatekeeper mechanism in skin tumorigenesis. Cancer Res 1997: **57**: 4677–4681.
43. Wicking C, Shanley S, Smyth I, Gillies S, Negus K, Graham S, Suthers G, Haites N, Edwards M, Wainwright B, Chenevix-Trench G. Most germ-line mutations in the nevoid basal cell carcinoma syndrome lead to a premature termination of the PATCHED protein, and no genotype-phenotype correlations are evident. Am J Hum Genet 1997: **60**: 21–26.
44. Wicking C, Smyth I, Bale A. The hedgehog signalling pathway in tumorigenesis and development. Oncogene 1999: **18**: 7844–7851.
45. Wolter M, Reifenberger J, Sommer C, Ruzicka T, Reifenberger G. Mutations in the human homologue of the *Drosophila* segment polarity gene patched (PTCH) in sporadic basal cell carcinomas of the skin and primitive neuroectodermal tumors of the central nervous system. Cancer Res 1997: **57**: 2581–2585.
46. Xie J, Murone M, Luoh SM, Ryan A, Gu Q, Zhang C, Bonifas JM, Lam CW, Hynes M, Goddard A, Rosenthal A, Epstein Jr EH, De Sauvage FJ. Activating smoothened mutations in sporadic basal-cell carcinoma. Nature 1998: **391**: 90–92.
47. Zedan W, Robinson PA, High AS. A novel polymorphism in the *PTC* gene allows easy identification of allelic loss in basal cell nevus syndrome lesions. Diagn Mol Pathol 2001: **10**: 41–45.

Address:
Kousuke Ohki
Department of Oral Medicine and Surgery
Division of Maxillofacial Surgery
Graduate School of Dentistry
Tohoku University
4-1 Seiryo-machi, Aoba-ku
Sendai 980-8575
Japan.
Tel: +81-22-717-8350;
Fax: +81-22-717-8304
E-mail: k-ohki@mail.tains.tohoku.ac.jp

Oral Microbiology Immunology 2004: 19: 379–385
Printed in Singapore. All rights reserved

Oral Microbiology and Immunology

Detection frequency of periodontitis-associated bacteria by polymerase chain reaction in subgingival and supragingival plaque of periodontitis and healthy subjects

G. Mayanagi[1], T. Sato[2], H. Shimauchi[1], N. Takahashi[2]
[1]Division of Periodontology and Endodontology, [2]Division of Oral Ecology and Biochemistry, Tohoku University Graduate School of Dentistry, Sendai, Japan

Mayanagi G, Sato T, Shimauchi H, Takahashi N. Detection frequency of periodontitis-associated bacteria by polymerase chain reaction in subgingival and supragingival plaque of periodontitis and healthy subjects.
Oral Microbiol Immunol 2004: 19: 379–385. © Blackwell Munksgaard, 2004.

The aim of this study was to compare the detection frequencies of 25 bacterial species in subgingival and supragingival plaque of 18 untreated periodontitis subjects and 12 periodontally healthy subjects. Genomic DNA was extracted from subgingival and supragingival plaque samples, and bacterial detection was performed by polymerase chain reaction of the 16S rRNA genes. Fourteen bacteria showed no relationship with periodontitis, and 11 of these 14 species were frequently detected (≥50%) in subgingival plaque in both periodontitis and healthy subjects. Nine bacteria such as *Eubacterium saphenum, Prevotella intermedia,* and *Treponema denticola* seemed to be related to periodontitis; their detection frequencies in subgingival plaque samples were higher in periodontitis than in healthy subjects, but these differences were not statistically significant by multiple comparisons ($0.002 \leq P < 0.05$). Two species (*Mogibacterium timidum* and *Porphyromonas gingivalis*) were detected significantly more frequently in subgingival plaque of periodontitis subjects than of healthy subjects ($P < 0.002$), with *P. gingivalis* being detected only in periodontitis subjects, suggesting that these two species are closely related to periodontitis. There were no significant differences in the detection frequencies of the 25 bacteria between subgingival and supragingival plaque, suggesting that the bacterial flora of supragingival plaque reflects that of subgingival plaque.

Key words: 16S rRNA genes; periodontitis; polymerase chain reaction; subgingival plaque; supragingival plaque

Nobuhiro Takahashi, DDS, PhD, Division of Oral Ecology and Biochemistry, Tohoku University Graduate School of Dentistry, Sendai 980–8575, Japan
Tel.: +81 22 717 8294;
fax: +81 22 717 8297;
e-mail: nobu-t@mail.tains.tohoku.ac.jp
Accepted for publication June 30, 2004

The composition of dental plaque microbiota in the human oral cavity is diverse and complex. It has been previously estimated by culturing and molecular biological methods that more than 600 species of bacteria inhabit the human oral cavity (13, 25, 27, 37, 49). The initiation and progression of periodontitis is thought to be caused by several species of these bacteria accumulating in subgingival periodontal pockets. *Porphyromonas gingivalis, Tannerella forsythia* (*Tannerella forsythensis*, formerly *Bacteroides forsythus*), and *Treponema denticola* are widely regarded as major periodontal pathogens (38), and numerous etiologic investigations of periodontal disease have therefore targeted these species. *Campylobacter rectus, Eikenella corrodens, Fusobacterium nucleatum, Micromonas micros* (formerly *Peptostreptococcus micros*), *Treponema amylovorum,*